3

Bifurcations Involving Fixed Points and Limit Cycles in Biological Systems

Michael R. Guevara

3.1 Introduction

Biological systems display many sorts of dynamic behaviors including constant behavior, simple or complex oscillations, and irregular fluctuating dynamics. As parameters in systems change, the dynamics may also also change. For example, changing the ionic composition of a medium bathing nerve cells or cardiac cells can have marked effects on the behaviors of these cells and may lead to the stabilization or destabilization of fixed points or the initiation or termination of rhythmic behaviors. This chapter concerns the ways that constant behavior and oscillating behavior can be stabilized or destabilized in differential equations. We give a summary of the mathematical analysis of bifurcations and biological examples that illustrate the mathematical concepts. While the context in which these bifurcations will be illustrated is that of low-dimensional systems of ordinary differential equations, these bifurcations can also occur in more complicated systems, such as partial differential equations and time-delay differential equations.

We first describe how fixed points can be created and destroyed as a parameter in a system of differential equations is gradually changed, producing a bifurcation. We shall focus on three different bifurcations: the saddle-node bifurcation, the pitchfork bifurcation, and the transcritical bifurcation (Abraham and Shaw 1982; Thompson and Stewart 1986; Wiggins 1990; Strogatz 1994).

We then consider how oscillations are born and how they die or metamorphose. There are several bifurcations in which limit cycles are created or destroyed. These include the Hopf bifurcation (see Chapter 2), the saddle-node bifurcation, the period-doubling bifurcation, the torus bifurcation, and the homoclinic bifurcation (Abraham and Shaw 1982; Thompson and Stewart 1986; Wiggins 1990; Strogatz 1994).

3.2 Saddle-Node Bifurcation of Fixed Points

3.2.1 Bistability in a Neural System

We now consider the case of "two stable resting potentials" as an example of a biological situation in which the number of fixed points in the system is changed as a parameter is varied. Normally, the voltage difference across the membrane of a nerve cell (the transmembrane potential) has a value at rest (i.e., when there is no input to the cell) of about −60 mV. Injecting a brief depolarizing current pulse produces an action potential: There is an excursion of the transmembrane potential, with the transmembrane potential asymptotically returning to the resting potential. This shows that there is a stable fixed point present in the system. However, it is possible under some experimental conditions to obtain two stable resting potentials. Figure 3.1 shows the effect of injection of a brief-duration stimulus pulse in an experiment in which a nerve axon is bathed in a potassium-rich medium: The transmembrane potential does not return to its resting value in response to delivery of a depolarizing stimulus pulse (the second stimulus pulse delivered in Figure 3.1); rather, it "hangs up" at a new depolarized potential, and rests there in a stable fashion (Tasaki 1959). This implies the existence of a second stable fixed point in the phase space of the system. Injection of a brief-duration current pulse of the opposite polarity (a hyperpolarizing stimulus pulse) can then return the membrane back to its initial resting potential (Tasaki 1959). In either case, the stimulus pulse must be large enough in amplitude for the flip to the other stable fixed point to occur; e.g., in Figure 3.1, the first stimulus pulse delivered was too small in amplitude to result in a flip to the other stable resting potential.

The phase space of the system of Figure 3.1 must also contain some sort of divider that separates the basins of attraction of the two stable fixed points (the **basin of attraction** of a fixed point is the set of initial conditions that asymptotically lead to that point). Figure 3.2 shows how this can occur in the simple one-dimensional system of ordinary differential equations $dx/dt = x - x^3$. In addition to the two stable fixed points at $x = \pm 1$, there is an unstable fixed point present at the origin, which itself acts to separate the basins of attraction of the two stable fixed points: trajectories starting from initial conditions to the left of the unstable fixed point at the origin (i.e., $x(t = 0) < 0$) go to the stable fixed point at $x = -1$, while trajectories starting from initial conditions to the right of that point (i.e., $x(t = 0) > 0$) go to the stable fixed point at $x = +1$.

The simplest way that the coexistence of two stable fixed points can occur in a two-dimensional system is shown in Figure 3.3, in which there is a saddle point in addition to the two stable nodes. Remember that the stable manifold of the saddle fixed point (the set of initial conditions that lead to it) is composed of a pair of **separatrices** (dashed lines in Figure 3.3), which divide the plane into two halves, forming the basins of attraction

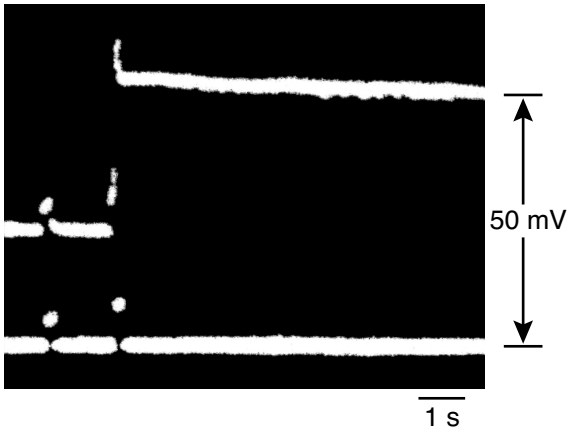

Figure 3.1. The phenomenon of two stable resting potentials in the membrane of a myelinated toad axon bathed in a potassium-rich medium. A steady hyperpolarizing bias current is injected throughout the experiment. Stimulation with a brief depolarizing current pulse that is large enough in amplitude causes the axon to go to a new level of resting potential. The top trace is the transmembrane potential; the bottom trace is the stimulus current. Adapted from Tasaki (1959).

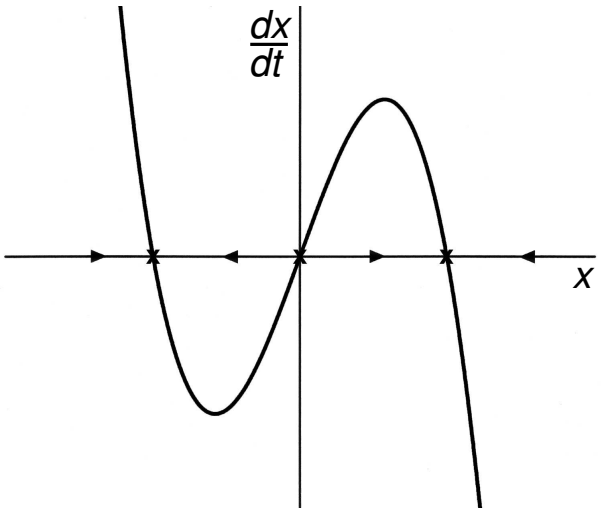

Figure 3.2. Coexistence of two stable fixed points in the one-dimensional ordinary differential equation $dx/dt = x - x^3$.

of the two stable fixed points. In Figure 3.3 the thick lines give the pair of trajectories that form the unstable manifold of the saddle point. From this phase-plane picture, can one explain why the pulse amplitude must be sufficiently large in Figure 3.1 for the transition from one resting potential

to the other to occur? Can one explain why a hyperpolarizing, and not depolarizing, stimulus pulse was used to flip the voltage back to the initial resting potential once it had been initially flipped to the more depolarized resting potential in Figure 3.1 by a depolarizing pulse?

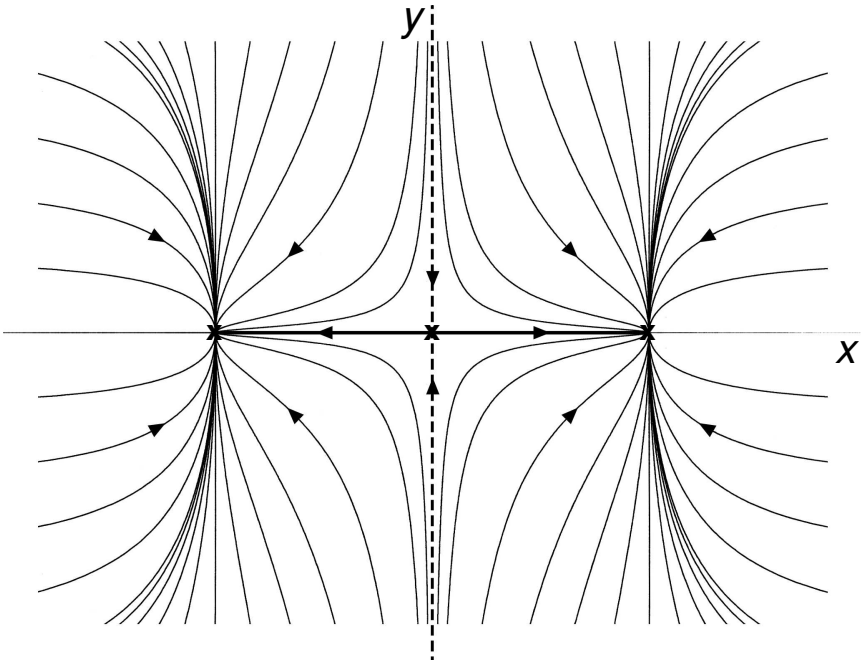

Figure 3.3. Coexistence of two stable nodes in a two-dimensional ordinary differential equation.

When the potassium concentration is normal, injection of a stimulus pulse into a nerve axon results in the asymptotic return of the membrane potential to the resting potential. There is thus normally only one fixed point present in the phase space of the system. It is clear from Figure 3.1 that elevating the external potassium concentration has produced a change in the number of stable fixed points present in the system. Let us now consider our first bifurcation involving fixed points: the saddle-node bifurcation. This bifurcation is almost certainly involved in producing the phenomenon of two stable resting potentials shown in Figure 3.1.

3.2.2 Saddle-Node Bifurcation of Fixed Points in a One-Dimensional System

In a one-dimensional system of ordinary differential equations, a **saddle-node bifurcation** results in the creation of two new fixed points, one

stable, the other unstable. This can be seen in the simple equation

$$\frac{dx}{dt} = \mu - x^2, \tag{3.1}$$

where x is the **bifurcation variable** and μ is the **bifurcation parameter**. Figure 3.4 illustrates the situation. For $\mu < 0$, there are no fixed points present in the system ($\mu = -0.5$ in Figure 3.4A). For $\mu = 0$ (**the bifurcation value**) there is one fixed point (at the origin), which is semistable (Figure 3.4B). For $\mu > 0$ there are two fixed points, one of which ($x^\star = \sqrt{\mu}$) is stable, while the other ($x^\star = -\sqrt{\mu}$) is unstable ($\mu = 0.5$ in Figure 3.4C). For obvious reasons, this bifurcation is also often called a **tangent bifurcation**.

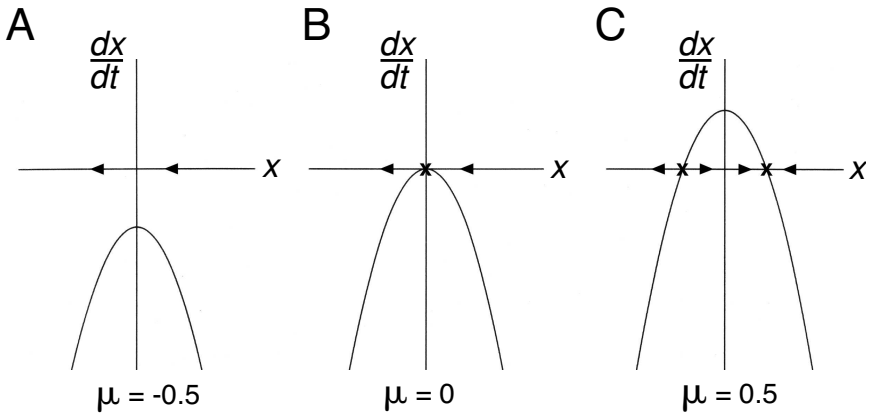

Figure 3.4. Saddle-node bifurcation in the one-dimensional ordinary differential equation of equation (3.1). (A) $\mu = -0.5$, (B) $\mu = 0$, (C) $\mu = 0.5$.

Figure 3.5 shows the corresponding bifurcation diagram, in which the equilibrium value ($x^\star$) of the bifurcation variable x is plotted as a function of the bifurcation parameter μ. The convention used is that stable points are shown as solid lines, while unstable points are denoted by dashed lines. In such a diagram, the point on the curve at which the saddle-node bifurcation occurs is often referred to as a **knee**, **limit point**, or **turning point**. This bifurcation is also called a **fold bifurcation** and is associated with one of the elementary catastrophes, the **fold catastrophe** (Arnold 1986; Woodcock and Davis 1978).

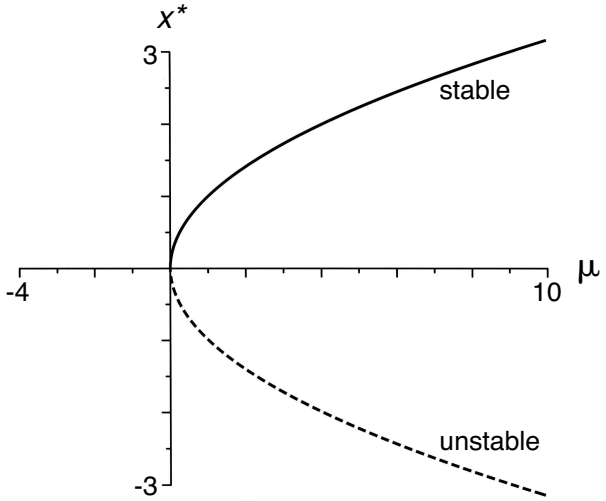

Figure 3.5. Bifurcation diagram for the saddle-node bifurcation occurring in equation (3.1).

3.2.3 Saddle-Node Bifurcation of Fixed Points in a Two-Dimensional System

Figure 3.6 shows the phase-plane portrait of the saddle-node bifurcation in a simple two-dimensional system of ordinary differential equations

$$\frac{dx}{dt} = \mu - x^2, \tag{3.2a}$$

$$\frac{dy}{dt} = -y. \tag{3.2b}$$

Again, for $\mu < 0$, there are no fixed points present in the system ($\mu = -0.5$ in Figure 3.6A); for $\mu = 0$ there is one, which is a saddle-node (Figure 3.6B); while for $\mu > 0$ there are two, which are a node and a saddle ($\mu = 0.5$ in Figure 3.6C), hence the name of the bifurcation. While in the particular example shown in Figure 3.6 the node is stable, the bifurcation can also be such that the node is unstable. This is in contrast to the one-dimensional case, where one cannot obtain two unstable fixed points as a result of this bifurcation. The bifurcation diagram for the two-dimensional case of Figure 3.6 is the same as that shown in Figure 3.5, which was for the one-dimensional case (Figure 3.4).

At the bifurcation point itself ($\mu = 0$), there is a special kind of fixed point, a **saddle-node**. This point has one eigenvalue at zero, the other necessarily being real (if negative, a stable node is the result of the bifurcation; if positive, an unstable node). In fact, this is the algebraic criterion for a saddle-node bifurcation: A single real eigenvalue passes through the origin in the root-locus diagram as a parameter is changed (Figures 3.4, 3.6). Note

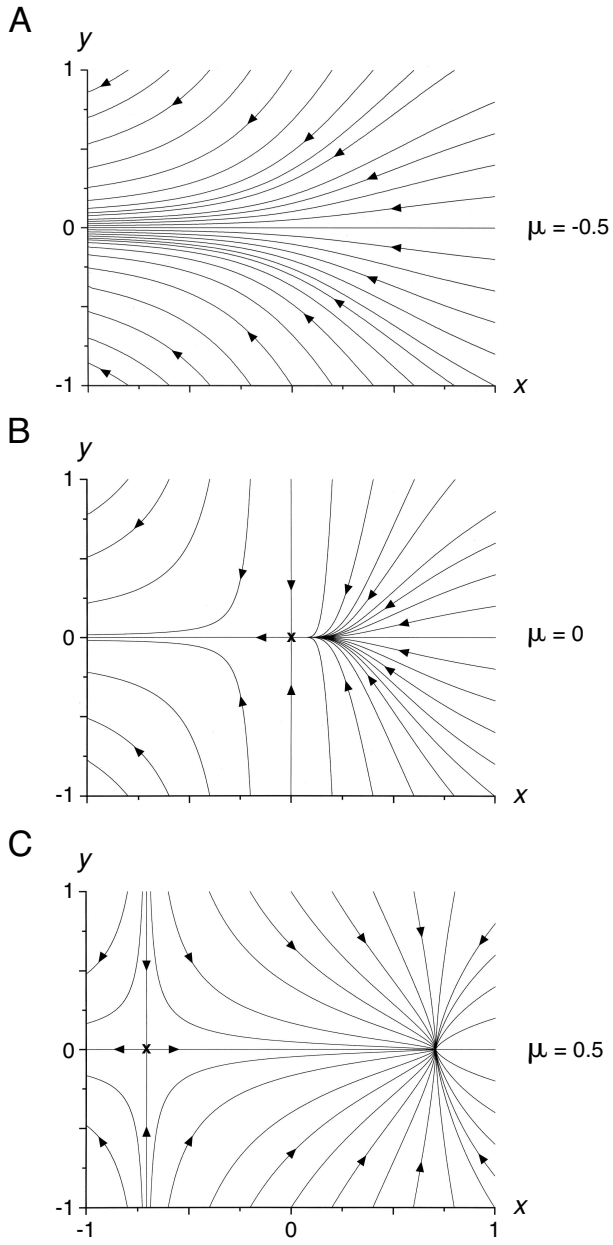

Figure 3.6. Phase-plane portrait of the saddle-node bifurcation in the two-dimensional ordinary differential equation of equation (3.2). (A) $\mu = -0.5$, (B) $\mu = 0$, (C) $\mu = 0.5$.

that the system is not structurally stable at the bifurcation value of the parameter; i.e., small changes in μ away from zero will cause qualitative changes in the phase-portrait of the system. In this particular case, such a change in parameter away from $\mu = 0$ would lead to the disappearance of the saddle-node ($\mu < 0$) or its splitting up into two fixed points ($\mu > 0$).

3.2.4 Bistability in a Neural System (Revisited)

After our brief excursion into the world of the saddle-node bifurcation, we now return to the question as to how the situation in Figure 3.1, with two stable resting potentials, arose from the normal situation in which there is only one resting potential. To investigate this further, we study the Hodgkin–Huxley model of the squid giant axon (Hodgkin and Huxley 1952).

Figure 3.7 gives the bifurcation diagram for the fixed points in the Hodgkin–Huxley model with the transmembrane voltage (V) being the bifurcation variable and the external potassium concentration (K_{out}) acting as the bifurcation parameter (Aihara and Matsumoto 1983). The model here is not one- or two-dimensional, as in Figures 3.2 to 3.6, but rather four-dimensional. The curve in Figure 3.7 gives the locus of the V-coordinate of the fixed points. As earlier, a solid curve indicates that the point is stable, while a dashed curve indicates that it is unstable. As K_{out} is increased in Figure 3.7, there is first a saddle-saddle bifurcation at the upper limit point (LP_u) at $K_{out} \approx 51.8$ mM that produces two saddle points (which, by definition, are inherently unstable). There is a second bifurcation at the lower limit point (LP_l) at $K_{out} \approx 417.0$ mM, which is a reverse saddle-node bifurcation that results in the coalescence and disappearance of a node and a saddle point. There is also a Hopf bifurcation (HB) at $K_{out} \approx 66.0$ mM that converts the stability of the fixed point created at LP_u from unstable to stable. There is thus quite a large range of K_{out} (66–417 mM) over which the phenomenon of two stable resting potentials can be seen. Remember that a fixed point in an N-dimensional system has N eigenvalues, which can be calculated numerically (e.g., using the `Auto` option in `XPP`*). At each of the two limit points or turning points in Figure 3.7, one of these eigenvalues, which is real, crosses the imaginary axis through the origin on the root-locus diagram.

3.2.5 Bistability in Visual Perception

Bistability, the coexistence in the phase space of the system of two asymptotically locally stable ("attracting") objects, is a phenomenon not limited

*See Appendix A for an introduction to `XPP`.

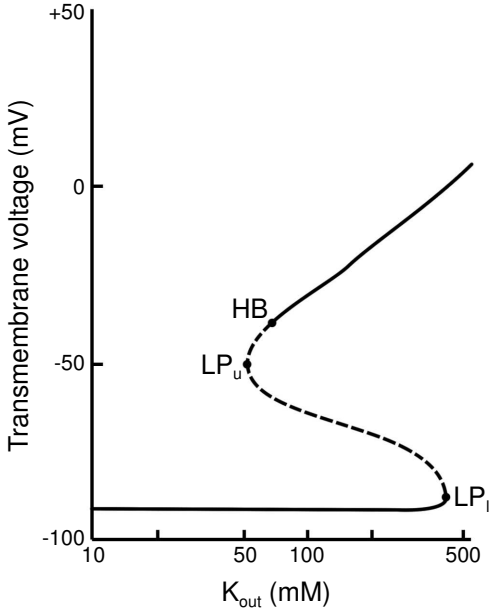

Figure 3.7. Bifurcation diagram for Hodgkin–Huxley model. The transmembrane voltage is the bifurcation variable, while the external potassium concentration (K_{out}) is the bifurcation parameter. As in the experimental work (Figure 3.1), a steady hyperpolarizing bias current (20 $\mu A/cm^2$ here) is injected throughout. Adapted from Aihara and Matsumoto (1983).

to fixed points. As we shall see later in this chapter, one can have bistability between a fixed point and a limit-cycle oscillator, which leads to the phenomena of single-pulse triggering and annihilation. In addition, one can have bistability between two stable periodic orbits (e.g., Abraham and Shaw 1982; Goldbeter and Martiel 1985; Guevara, Shrier, and Glass 1990; Yehia, Jeandupeux, Alonso, and Guevara 1999). Thus, many other phenomena in which two stable behaviors are seen in experimental work are almost certainly due to the coexistence of two stable attractors of some sort. The most appealing example of this is perhaps in the field of visual perception, where one can have bistable images. Figure 3.8 shows a nice example, in which the relative size of the basins of attraction for the perception of the two figures gradually changes as one moves from left to right.

Figure 3.8. Bistability in visual perception. Adapted from Chialvo and Apkarian (1993).

At the extreme ends of the sequence of images in Figure 3.8, only one figure is perceived, while in the middle the eye perceives one of two figures at a given time ("ambiguous figure"). Thus, Figure 3.9 shows a candidate bifurcation diagram, in which there are two saddle-node bifurcations, so that one perceives only one figure or the other at the two extremes of the diagram. The phenomenon of hysteresis also occurs: Scan the sequence of images in Figure 3.8 from left to right and note at which image the transition from the male face to the female form is perceived. Then repeat, reversing the direction of scanning, so that one now scans from right to left. Is there a difference? How does the schematic bifurcation diagram of Figure 3.9 explain this?

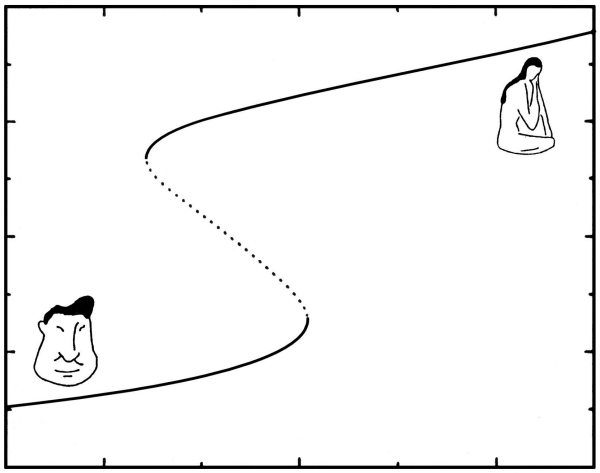

Figure 3.9. Candidate bifurcation diagram for hysteresis in visual perception.

3.3 Pitchfork Bifurcation of Fixed Points

3.3.1 Pitchfork Bifurcation of Fixed Points in a One-Dimensional System

In the **pitchfork bifurcation**, a fixed point reverses its stability, and two new fixed points are born. A pitchfork bifurcation occurs at $\mu = 0$ in the one-dimensional ordinary differential equation

$$\frac{dx}{dt} = x(\mu - x^2). \tag{3.3}$$

For $\mu < 0$, there is one fixed point at zero, which is stable ($\mu = -0.5$ in Figure 3.10A); at $\mu = 0$ there is still one fixed point at zero, which is still

stable (Figure 3.10B); for $\mu > 0$, there are three fixed points, with the original fixed point at zero now being unstable, and the two new symmetrically placed points being stable ($\mu = 0.5$ in Figure 3.10C).

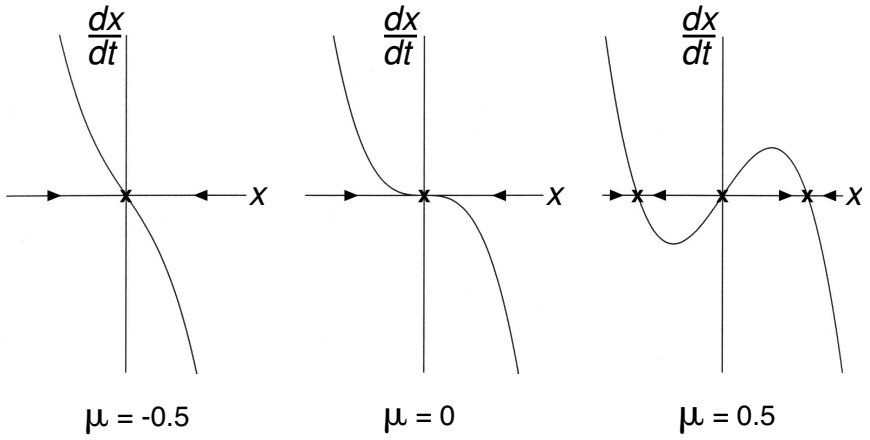

Figure 3.10. Pitchfork bifurcation in the one-dimensional system of equation (3.3). (A) $\mu = -0.5$, (B) $\mu = 0$, (C) $\mu = 0.5$.

Figure 3.11 shows the bifurcation diagram for the pitchfork bifurcation. The bifurcation of Figures 3.10, 3.11 is **supercritical pitchfork bifurcation**, since there are stable fixed points to either side of the bifurcation point. Replacing the minus sign with a plus sign in equation (3.3) results in a **subcritical** pitchfork bifurcation.

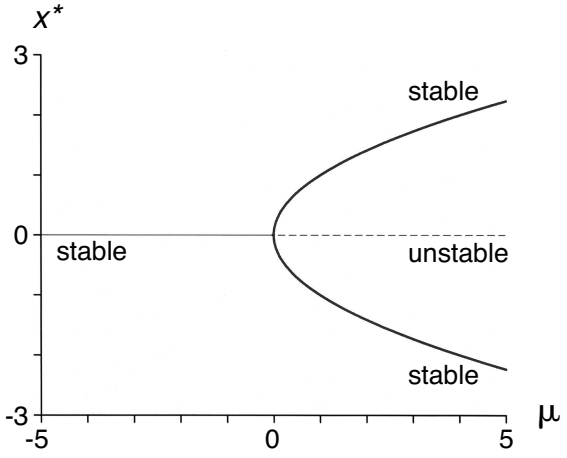

Figure 3.11. Bifurcation diagram for the pitchfork bifurcation.

3.3.2 Pitchfork Bifurcation of Fixed Points in a Two-Dimensional System

There is a **pitchfork bifurcation** at $\mu = 0$ for the two-dimensional system of ordinary differential equations

$$\frac{dx}{dt} = x(\mu - x^2), \tag{3.4a}$$

$$\frac{dy}{dt} = -y. \tag{3.4b}$$

For $\mu < 0$, there is one fixed point, which is a stable node ($\mu = -0.5$ in Figure 3.12A); at $\mu = 0$ there is still only one fixed point, which remains a stable node (Figure 3.12B); for $\mu > 0$, there are three fixed points, with the original fixed point at zero now being a saddle point, and the two new symmetrically placed points being stable nodes ($\mu = 0.5$ in Figure 3.12C). The bifurcation diagram is the same as that shown in Figure 3.11.

3.3.3 The Cusp Catastrophe

So far, we have generally considered one-parameter bifurcations, in which we have changed a single bifurcation parameter μ. Let us now introduce a second bifurcation parameter ϵ into the one-dimensional equation producing the pitchfork bifurcation, equation (3.3), studying instead

$$\frac{dx}{dt} = x(\mu - x^2) + \epsilon. \tag{3.5}$$

Figure 3.13 gives the resultant two-parameter bifurcation diagram, in which the vertical axis gives the equilibrium value ($x^\star$) of the bifurcation variable x, while the other two axes represent the two bifurcation parameters (μ and ϵ). Thus, at a given combination of μ and ϵ, $x^\star$ is given by the point(s) lying in the surface directly above that combination. There are therefore values of (μ, ϵ) where there are three fixed points present. These combinations are found within the cusp-shaped cross-hatched region illustrated in the (μ, ϵ) parameter plane. For (μ, ϵ) combinations outside of this region, there is only one fixed point. Choosing a bifurcation route (i.e., a curve lying in the (μ, ϵ) parameter plane) that runs through either of the curves forming the cusp in that plane results in a saddle-node bifurcation. Choosing a bifurcation route that runs through the cusp itself results in a pitchfork bifurcation. It is now clear why, if there is a pitchfork bifurcation as μ is changed for $\epsilon = 0$, there will be a saddle-node bifurcation when μ is changed for $\epsilon \neq 0$. Viewed as a one-parameter bifurcation, the pitchfork bifurcation in one dimension is thus unstable with respect to small perturbations.

There has been much speculation on the role of the cusp catastrophe in phenomena encountered in many areas of life, including psychiatry, economics, sociology, and politics (see, e.g., Woodcock and Davis 1978).

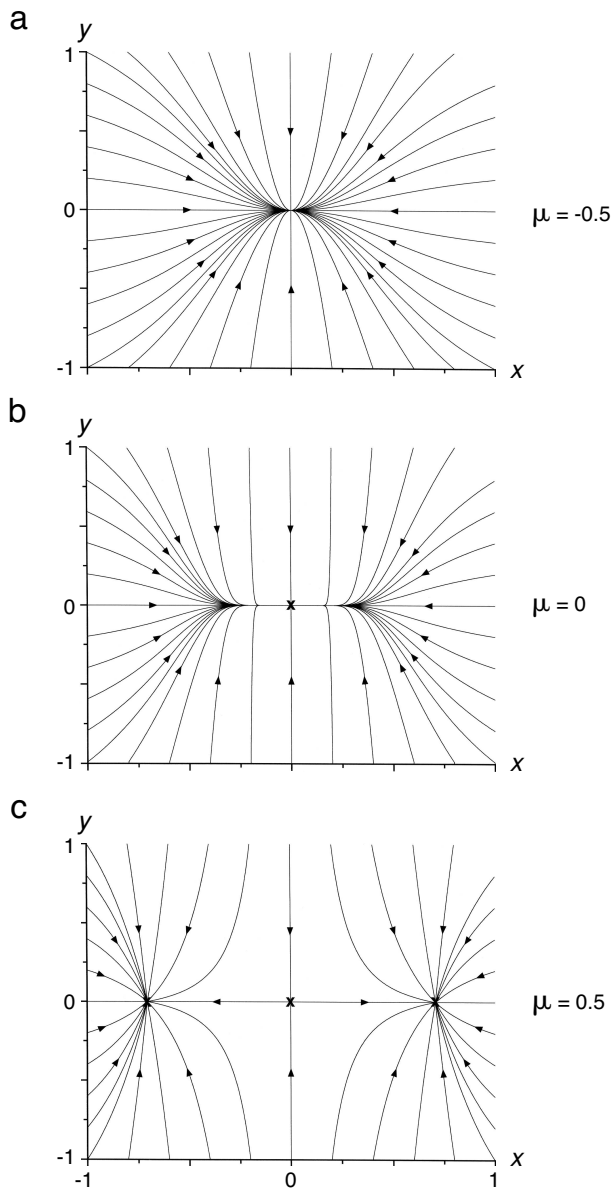

Figure 3.12. Phase-plane portrait of the pitchfork bifurcation in the two-dimensional ordinary differential equation of equation (3.4). (A) $\mu = -0.5$, (B) $\mu = 0$, (C) $\mu = 0.5$.

3.4 Transcritical Bifurcation of Fixed Points

3.4.1 Transcritical Bifurcation of Fixed Points in a One-Dimensional System

In the **transcritical bifurcation** there is an exchange of stability between two fixed points. In the one-dimensional ordinary differential equation

$$\frac{dx}{dt} = x(\mu - x), \tag{3.6}$$

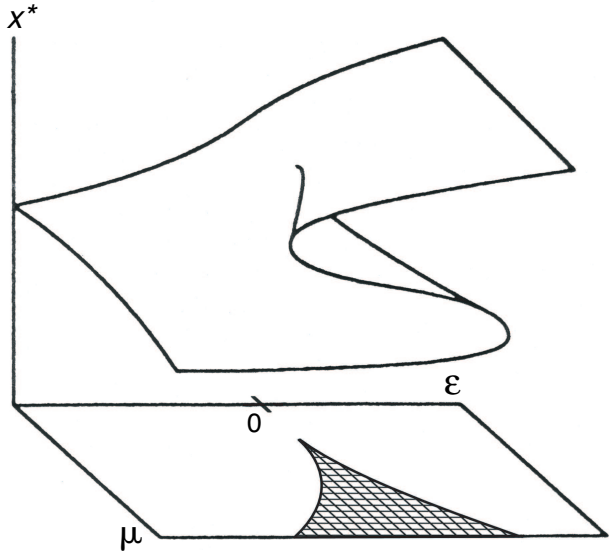

Figure 3.13. The pitchfork bifurcation in the two-parameter unfolding of equation (3.5). Adapted from Strogatz (1994).

there is a transcritical bifurcation at $\mu = 0$ (Figure 3.14). The fixed point at $x^\star = 0$ starts out being stable for $\mu < 0$ ($\mu = -0.5$ in Figure 3.14A), becomes semistable at $\mu = 0$ (Figure 3.14B), and is then unstable for $\mu > 0$ ($\mu = -0.5$ in Figure 3.14C). The sequence of changes is the opposite for the other fixed point ($x^\star = \mu$). Figure 3.15 gives the bifurcation diagram.

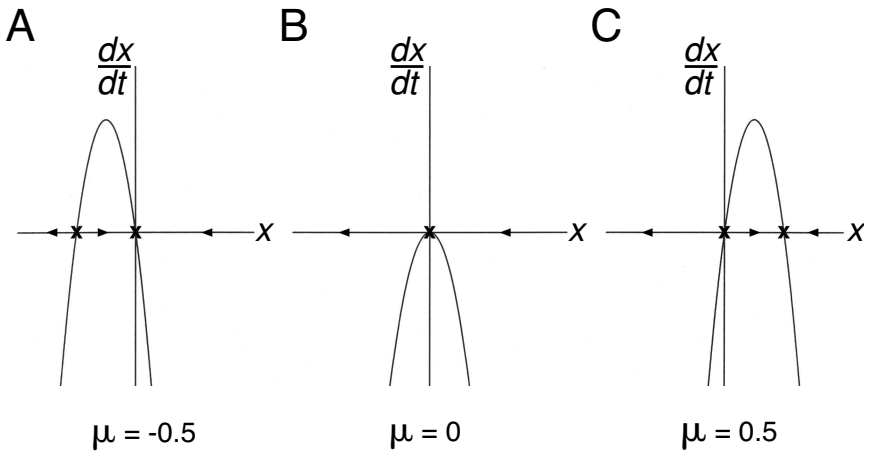

Figure 3.14. Transcritical bifurcation in the one-dimensional ordinary differential equation of equation (3.6). (A) $\mu = -0.5$, (B) $\mu = 0$, (C) $\mu = 0.5$.

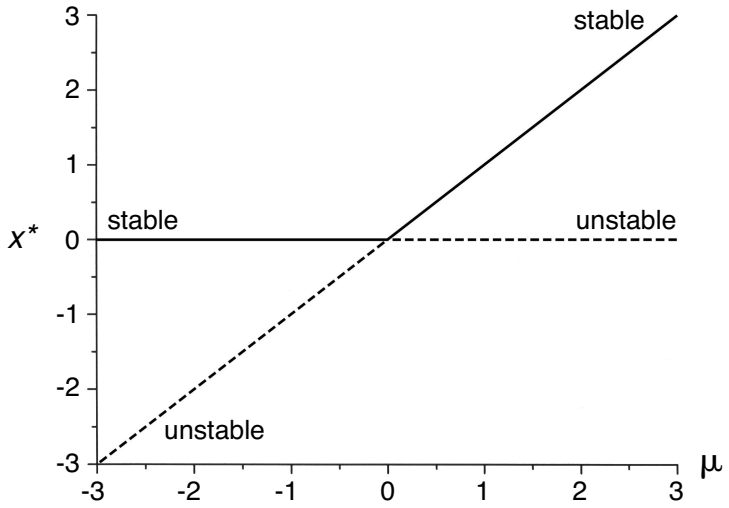

Figure 3.15. The bifurcation diagram for the transcritical bifurcation of equation (3.6).

As in the case of the pitchfork bifurcation, the transcritical bifurcation in a one-dimensional system (Figure 3.14) is not stable to small perturbations, in that should a term ϵ be added to the right-hand side of equation (3.6), the transcritical bifurcation ($\epsilon = 0$) is replaced by either no bifurcation at all ($\epsilon > 0$) or by a pair of saddle-node bifurcations ($\epsilon < 0$) (Wiggins 1990).

3.4.2 Transcritical Bifurcation of Fixed Points in a Two-Dimensional System

The two-dimensional ordinary differential equation

$$\frac{dx}{dt} = x(\mu - x), \tag{3.7a}$$

$$\frac{dy}{dt} = -y, \tag{3.7b}$$

also has a transcritical bifurcation at $\mu = 0$ (Figure 3.16). The fixed point at $x^\star = 0$ starts out being a stable node for $\mu < 0$ ($\mu = -0.5$ in Figure 3.16A), becomes a semistable saddle-node at $\mu = 0$ (Figure 3.16B), and is then an unstable saddle point for $\mu > 0$ ($\mu = 0.5$ in Figure 3.16C). The sequence of changes is the opposite for the other fixed point ($x^\star = \mu$). As with the saddle-node bifurcation (Figure 3.6), the fixed point present at the bifurcation point ($\mu = 0$) is a saddle-node.

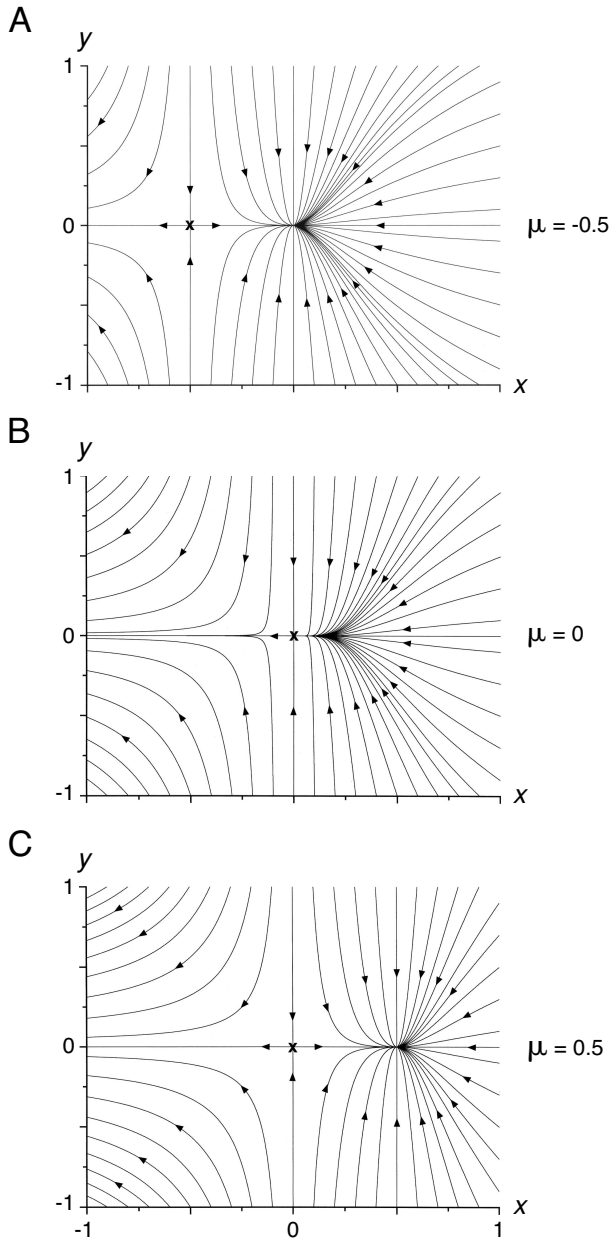

Figure 3.16. Phase-plane portrait of the transcritical bifurcation for the two-dimensional ordinary differential equation of equation (3.7). (A) $\mu = -0.5$, (B) $\mu = 0$, (C) $\mu = 0.5$.

3.5 Saddle-Node Bifurcation of Limit Cycles

3.5.1 Annihilation and Single-Pulse Triggering

The sinoatrial node is the pacemaker that normally sets the rate of the heart. Figure 3.17 shows the transmembrane potential recorded from a cell within the sinoatrial node. At the arrow, a subthreshold pulse of current is delivered to the node, and spontaneous activity ceases. This phenomenon is termed **annihilation**. Injection of a suprathreshold current pulse will then restart activity (**"single-pulse triggering"**). Both of these phenomena can be seen in an ionic model of the sinoatrial node: Figure 3.18A shows annihilation, while Figure 3.18B shows single-pulse triggering.

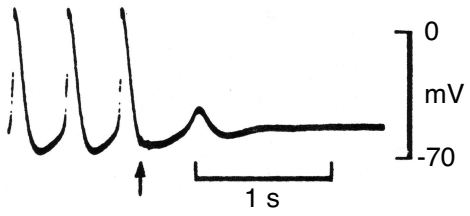

Figure 3.17. Annihilation in tissue taken from the sinoatrial node. From Jalife and Antzelevitch (1979).

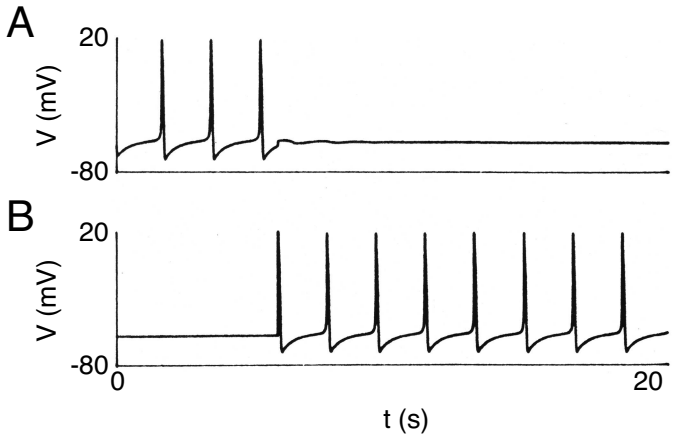

Figure 3.18. (A) Annihilation and (B) single-pulse triggering in an ionic model of the sinoatrial node. A constant hyperpolarizing bias current is injected to slow the beat rate. From Guevara and Jongsma (1992).

Annihilation has been described in several other biological oscillators, including the eclosion rhythm of fruit flies, the circadian rhythm of bioluminescence in marine algae, and biochemical oscillators (see Winfree 2000 for a

synopsis). Figure 3.19 shows another example taken from electrophysiology. When a constant ("bias") current is injected into a squid axon, the axon will start to spontaneously generate action potentials (Figure 3.19A). Injection of a well-timed pulse of current of the correct amplitude annihilates this spontaneous activity (Figure 3.19B).

Figure 3.19. (A) Induction of periodic firing of action potentials in the giant axon of the squid by injection of a depolarizing bias current. (B) Annihilation of that bias-current-induced activity by a brief stimulus pulse. V = transmembrane voltage, I = injected current. From Guttman, Lewis, and Rinzel (1980).

Annihilation can also be seen in the Hodgkin–Huxley equations (Hodgkin and Huxley 1952), which are a four-dimensional system of ordinary differential equations modeling electrical activity in the membrane of the giant axon of the squid (see Chapter 4). Note that the phase of the cycle at which annihilation can be obtained depends on the polarity of the stimulus (Figure 3.20A vs. Figure 3.20B).

3.5.2 Topology of Annihilation and Single-Pulse Triggering

The fact that one can initiate or terminate spontaneous activity by injection of a brief stimulus pulse means that there is the coexistence of two stable attractors in the system. One is a stable fixed point, corresponding to rest or quiescence; the other is a stable limit-cycle oscillator, corresponding to spontaneous activity. The simplest topology that is consistent with this requirement is shown in Figure 3.21A. Starting from initial condition *a* or *b*, the state point asymptotically approaches the stable limit cycle (*solid curve*), while starting from initial condition *c*, the stable fixed point is approached. The unstable limit cycle (*dashed curve*) in this two-dimensional system is thus a separatrix that divides the plane into the

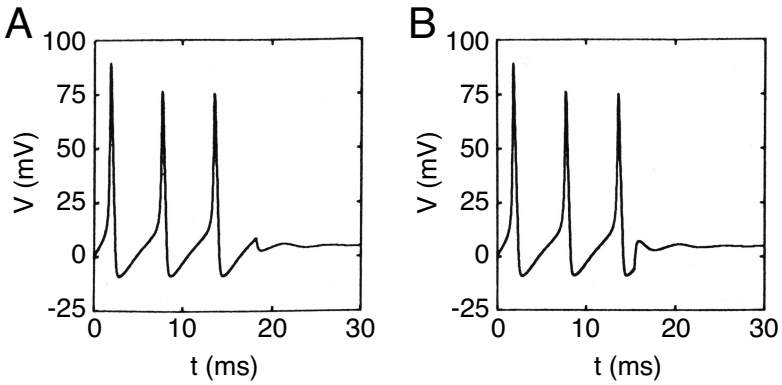

Figure 3.20. Annihilation of bias-current-induced spontaneous activity in the Hodgkin–Huxley equations by a current-pulse stimulus. (A) Hyperpolarizing, (B) depolarizing current pulse. The convention that the resting membrane potential is 0 mV is taken. From Guttman, Lewis, and Rinzel (1980).

basins of attraction of the stable fixed point and the stable limit cycle. In a higher-dimensional system, it is the stable manifold of the unstable limit cycle that can act as a separatrix, since the limit cycle itself, being a one-dimensional object, can act as a separatrix only in a two-dimensional phase space.

In Figure 3.21B, the state point is initially sitting at the stable fixed point, producing quiescence in the system. Injecting a brief stimulus of large enough amplitude will knock the state point to the point *d*, allowing it to escape from the basin of attraction of the fixed point and enter into the basin of attraction of the stable limit cycle. Periodic activity will then be seen. Figure 3.21B thus explains why the stimulus pulse must be of some minimum amplitude to trigger spontaneous activity. Figure 3.21C shows the phenomenon of annihilation. During spontaneous activity, at the point in the cycle when the state point is at *e*, a stimulus is injected that takes the state point of the system to point *f*, which is within the basin of attraction of the stable fixed point (**black hole** in the terminology of Winfree 1987). Spontaneous activity is then asymptotically extinguished. One can appreciate from this figure that for annihilation to be successful, the stimulus must be delivered within a critical window of timing, and that the location of this window will change should the polarity, amplitude, or duration of the stimulus pulse be changed. One can also see that the stimulus pulse must be of some intermediate amplitude to permit annihilation of spontaneous activity.

The phenomena of annihilation and single-pulse triggering are not seen in all biological oscillators. For example, one would think that it might not be a good idea for one's sinoatrial node to be subject to annihilation. Indeed, there are other experiments on the sinoatrial node that indicate

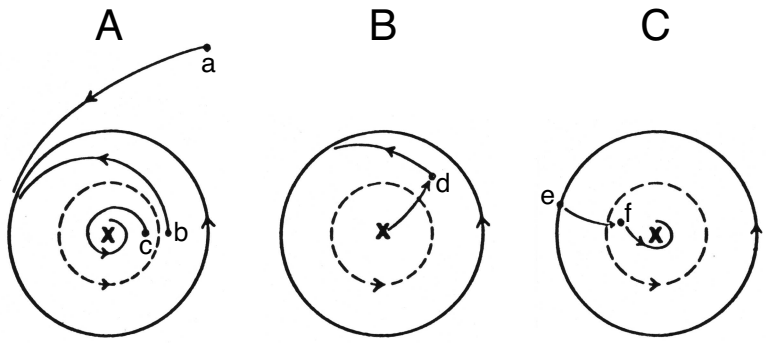

Figure 3.21. (A) System with coexisting stable fixed point (x) and stable limit cycle oscillation (*solid closed curve*). Dashed closed curve is an unstable limit-cycle oscillation. (B) Single-pulse triggering. (C) Annihilation. From Guevara and Jongsma (1992).

that there is only one fixed point present, and that this point is unstable (Figure 3.22). Thus, these other experiments suggest that the sinoatrial node belongs to the class of oscillators with the simplest possible topology: There is a single limit cycle, which is stable, and a single fixed point, which is unstable. This topology does not allow triggering and annihilation. The question thus naturally arises as to how the topology of Figure 3.21A can originate. There are several such ways, one of which involves a saddle-node bifurcation of periodic orbits, which we shall now discuss.

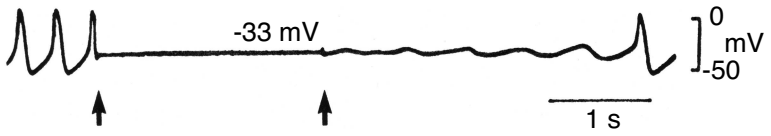

Figure 3.22. Clamping the transmembrane potential of a spontaneously beating piece of tissue taken from the sinoatrial node to its equilibrium value (*first arrow*) and then releasing the clamp (*second arrow*) results in the startup of spontaneous activity, indicating that the fixed point is unstable. From Noma and Irisawa (1975).

3.5.3 Saddle-Node Bifurcation of Limit Cycles

In a **saddle-node bifurcation of limit cycles**, there is the creation of a pair of limit cycles, one stable, the other unstable. Figure 3.23 illustrates this bifurcation in the two-dimensional system of ordinary differential

equations, written in polar coordinates (Strogatz 1994)

$$\frac{dr}{dt} = \mu r + r^3 - r^5, \tag{3.8a}$$

$$\frac{d\theta}{dt} = \omega + br^3. \tag{3.8b}$$

The first equation above can be rewritten as $dr/dt = r(\mu + r^2 - r^4)$, which has roots at $r^\star = 0$ and at $r^\star = [(1 \pm (1+4\mu)^{1/2})/2]^{1/2}$. The solution $r^\star = 0$ corresponds to a fixed point. For $\mu < -\frac{1}{4}$, the two other roots are complex, and there are no limit cycles present (Figure 3.23A). At the bifurcation point ($\mu = -\frac{1}{4}$), there is the sudden appearance of a limit cycle of large (i.e., nonzero) amplitude with $r^\star = 1/\sqrt{2}$ (Figure 3.23B). This limit cycle is semistable, since it attracts trajectories starting from initial conditions exterior to its orbit, but repels trajectories starting from initial conditions lying in the interior of its orbit. For $\mu > -\frac{1}{4}$ (Figure 3.23C), there are two limit cycles present, one stable (at $r^\star = [(1 + (1 + 4\mu)^{1/2})/2]^{1/2}$) and the other unstable (at $r^\star = [(1 - (1 - 4\mu)^{1/2})/2]^{1/2}$).

Figure 3.24 gives the bifurcation diagram for the saddle-node bifurcation of periodic orbits. When plotting such a diagram, one plots some characteristic of the limit cycle (such as the peak-to-peak amplitude of one variable, or the maximum and/or minimum values of that variable) as a function of the bifurcation parameter. In Figure 3.24, the diameter of the circular limit cycles of Figure 3.23 (which amounts to the peak-to-peak amplitude) is plotted as a function of the bifurcation parameter.

3.5.4 Saddle-Node Bifurcation in the Hodgkin–Huxley Equations

Let us now return to our example involving annihilation in the Hodgkin–Huxley equations (Figure 3.20). Figure 3.25 shows the projection on the Vn-plane of trajectories in the system (V and n are two of the variables in the four-dimensional system). With no bias current (I_{bias}), there is a stable fixed point present. In this situation, injection of a single stimulus pulse produces an action potential. As a bias current is injected, one has a saddle-node bifurcation at $I_{\text{bias}} \approx 8.03\ \mu\text{A/cm}^2$. Just beyond this saddle-node bifurcation (Figure 3.25A), there are two stable structures present, a stable fixed point and a stable limit cycle (the outer closed curve) that produces spontaneous firing of the membrane, as well as one unstable structure, an unstable limit cycle (the inner closed curve). As I_{bias} is increased, the unstable limit cycle shrinks in size (Figure 3.25B,C,D), until at $I_{\text{bias}} \approx 18.56\ \mu\text{A/cm}^2$, there is a subcritical Hopf bifurcation (see Chapter 2) in which the unstable limit cycle disappears and the stable fixed point becomes unstable. Still further increase of I_{bias} leads to a shrinkage in the size of the stable limit cycle. Eventually, another Hopf bifurcation,

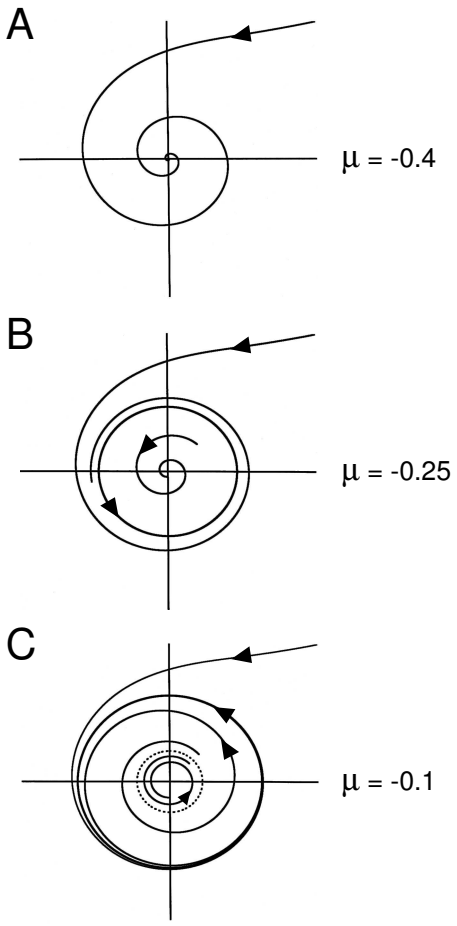

Figure 3.23. The saddle-node bifurcation of limit cycles in the two-dimensional system of ordinary differential equations given by equation 3.8. (A) $\mu = -0.4$, (B) $\mu = -0.25$, (C) $\mu = -0.1$.

which is supercritical, occurs at $I_{\text{bias}} \approx 154.5\ \mu\text{A/cm}^2$, resulting in the disappearance of the stable limit cycle and the conversion of the unstable fixed point into a stable fixed point. Beyond this point, there is no periodic activity.

Figure 3.26 gives the bifurcation diagram for the behavior shown in Figure 3.25, computed with `XPP`.[†] One consequence of this diagram is that single-pulse triggering will occur only over an intermediate range of I_{bias} ($8.03\ \mu\text{A/cm}^2 < I_{\text{bias}} < 18.56\ \mu\text{A/cm}^2$). This is due to the fact that for

[†]See Appendix A for an introduction to `XPP`.

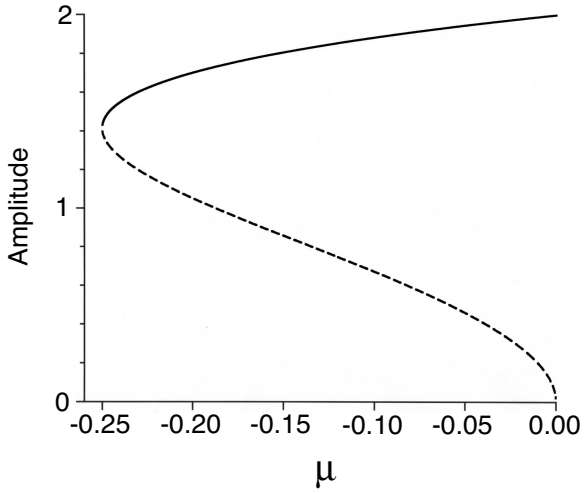

Figure 3.24. Bifurcation diagram for limit cycles in the saddle-node bifurcation of periodic orbits shown in Figure 3.23.

$I_{\text{bias}} < 8.03\ \mu\text{A/cm}^2$ there are no limit cycles present in the system, while for $18.56\ \mu\text{A/cm}^2 < I_{\text{bias}} < 154.5\ \mu\text{A/cm}^2$ the fixed point is unstable, and for $I_{\text{bias}} > 154.5\ \mu\text{A/cm}^2$, there are again no limit cycles present. There are thus, in this example, two routes by which the topology allowing annihilation and single-pulse triggering ($8.03\ \mu\text{A/cm}^2 < I_{\text{bias}} < 18.56\ \mu\text{A/cm}^2$) can be produced: (i) As I_{bias} is increased from a very low value, there is a single saddle-node bifurcation; (ii) as I_{bias} is reduced from a very high value, there are two Hopf bifurcations, the first supercritical, the second subcritical.

3.5.5 Hysteresis and Hard Oscillators

Another consequence of the bifurcation diagram of Figure 3.26 is that there will be hysteresis in the response to injection of a bias current. This has been investigated experimentally in the squid axon. When a ramp of current is injected into the squid axon, firing will start at a value of bias current that is higher than the value at which firing will stop as the current is ramped down (Figure 3.27). Oscillators such as that shown in Figure 3.27 that start up at large amplitude as a parameter is slowly changed are said to be "**hard**," whereas those that start up at zero amplitude (i.e., via a supercritical Hopf bifurcation) are said to be "**soft**."

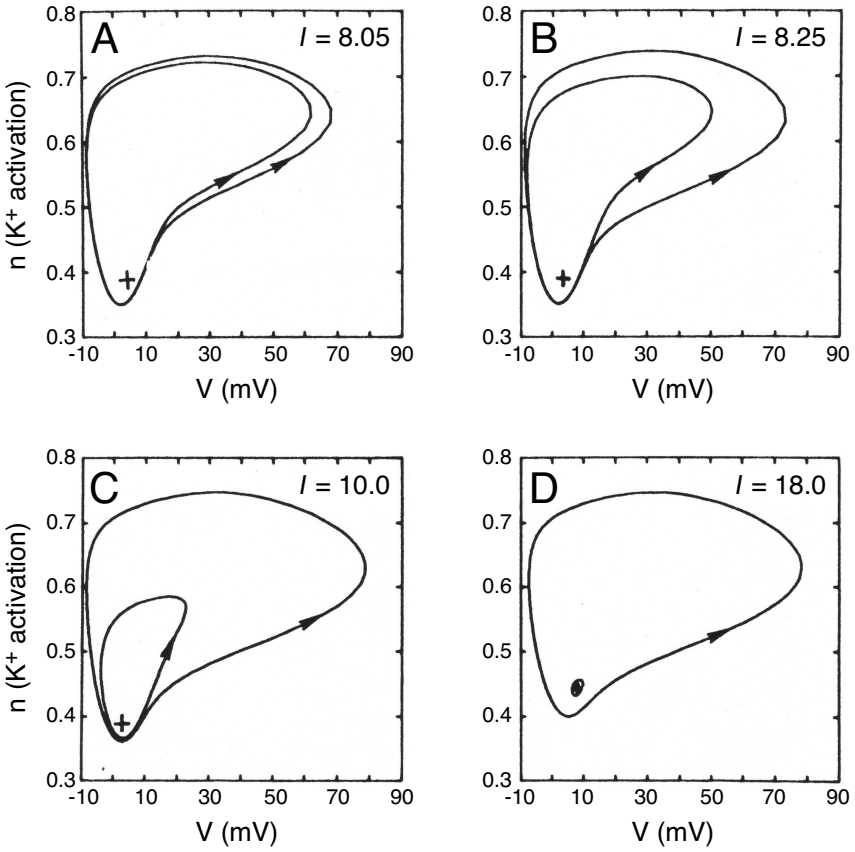

Figure 3.25. Phase-plane portrait of Hodgkin–Huxley equations as bias current I_{bias} is changed. The convention that the normal resting potential is 0 mV is taken. Adapted from Guttman, Lewis, and Rinzel (1980).

3.5.6 Floquet Multipliers at the Saddle-Node Bifurcation

Let us now analyze the saddle-node bifurcation of Figure 3.23 by taking Poincaré sections and examining the resultant Poincaré first-return maps. In this case, since the system is two-dimensional, the Poincaré surface of section (Π) is a one-dimensional curve, and the Poincaré map is one-dimensional. At the bifurcation point, where a semistable orbit exists, one can see that there is a tangent or saddle-node bifurcation on the Poincaré map (Figure 3.28A). Beyond the bifurcation point, there is a stable fixed point on the map, corresponding to the stable limit cycle, and an unstable fixed point on the map, corresponding to the unstable limit cycle (Figure 3.28B). Remembering that the slope of the map at the fixed point gives the Floquet multiplier, one can appreciate that a saddle-node

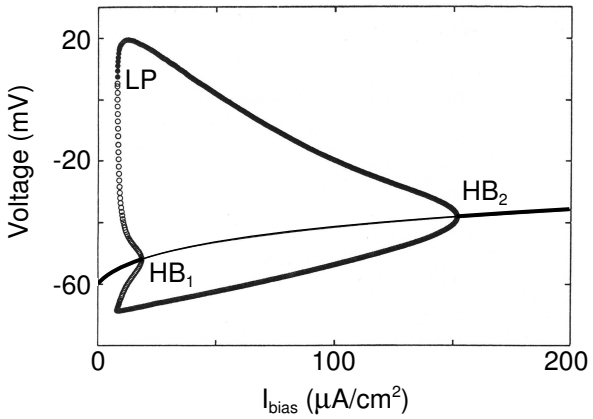

Figure 3.26. Bifurcation diagram for response of Hodgkin–Huxley equations to a bias current (I_{bias}), computed using `XPP`. *Thick curve*: stable fixed points; *thin curve*: unstable fixed points; *filled circles*: stable limit cycles; *unfilled circles*: unstable limit cycles.

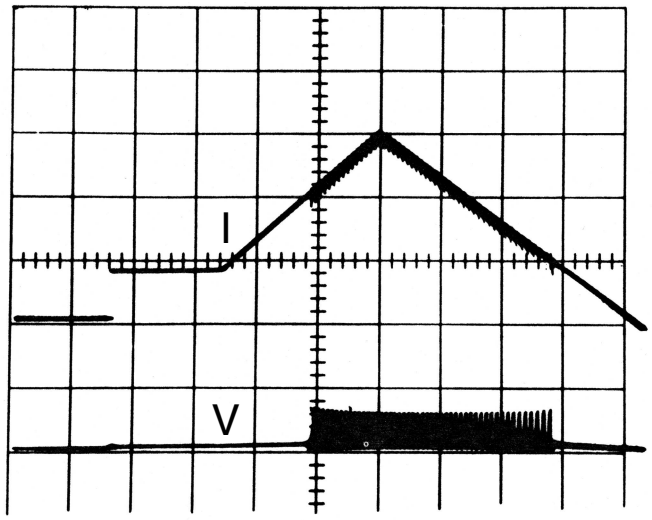

Figure 3.27. Hysteresis in the response of the squid axon to injection of a ramp of bias current. V = transmembrane potential, I = injected bias current. From Guttman, Lewis, and Rinzel (1980).

bifurcation occurs when a real Floquet multiplier moves through +1 on the unit circle.

When the saddle-node bifurcation of limit cycles occurs in a three-dimensional system, the stable limit cycle is a nodal cycle and the unstable limit cycle is a saddle cycle (Figure 3.29). The Poincaré plane of section

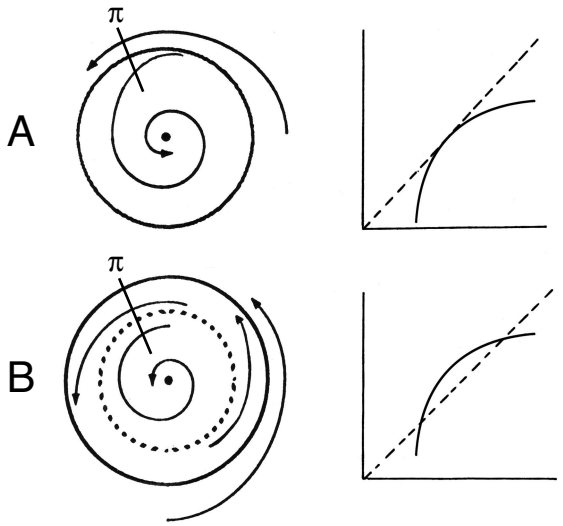

Figure 3.28. Saddle-node bifurcation in a two-dimensional system. Poincaré section (surface of section indicated by Π) and Poincaré return map: (A) at the bifurcation point, (B) beyond the bifurcation point.

and the Poincaré map are then both two-dimensional. As the bifurcation point is approached, moving in the reverse direction, the two limit cycles in Figure 3.29 approach one another, eventually coalescing into a saddle-nodal cycle, which then disappears, hence the name of the bifurcation. In the Poincaré sections, this corresponds to the nodal fixed point coalescing with the saddle point, producing a saddle-node fixed point. The result is a saddle-node bifurcation of fixed points. Examining the Floquet multipliers associated with the two cycles in Figure 3.29, one can see that the bifurcation again occurs when a Floquet multiplier moves through +1 on the unit circle. Just as a saddle-node bifurcation of fixed points can also produce an unstable node and a saddle point, the saddle-node bifurcation of limit cycles can also result in the appearance of an unstable nodal cycle and a saddle cycle.

3.5.7 Bistability of Periodic Orbits

We have previously considered situations in which two stable fixed points can coexist. It is also possible to have coexistence of two stable limit cycles. An example of this is shown in Figure 3.30A, in which a single cell isolated from the rabbit ventricle is driven with a train of current pulse stimuli delivered at a relatively fast rate. At the beginning of the trace, there is 1:1 synchronization between the train of stimulus pulses and the action potentials. This periodic behavior corresponds to a limit cycle in the phase

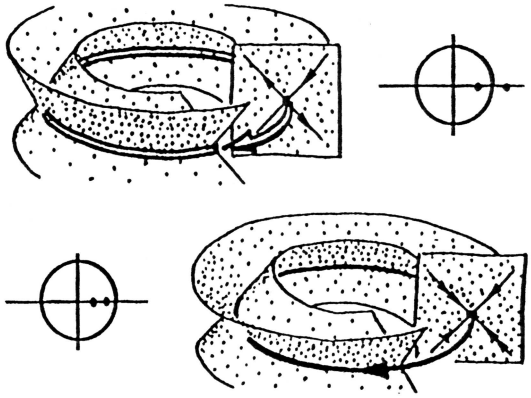

Figure 3.29. Saddle (top) and nodal (bottom) limit cycles produced by saddle-node bifurcation in a three-dimensional system. Adapted from Abraham and Shaw (1982).

space of the system. At the arrow, a single extra stimulus pulse is delivered. This extra stimulus flips the 1:1 rhythm to a 2:1 rhythm, in which every second stimulus produces only a subthreshold response. Similar behavior can be seen in an ionic model of ventricular membrane (Figure 3.30B).

There are thus two stable rhythms that coexist, with one or the other being seen, depending on initial conditions. It is also possible to flip from the 1:1 to the 2:1 rhythm by dropping pulses from the basic drive train, as well as to flip from the 2:1 rhythm back to the 1:1 rhythm by inserting an extra stimulus with the correct timing (Yehia, Jeandupeux, Alonso, and Guevara 1999). Similar results have also been described in the quiescent dog ventricle (Mines 1913) and in aggregates of spontaneously beating embryonic chick ventricular cells (Guevara, Shrier, and Glass 1990).

The existence of bistability means that hysteresis can be seen: The transition from 1:1 to 2:1 rhythm does not occur at the same driving frequency as the reverse transition from 2:1 to 1:1 rhythm. A systematic study of this phenomenon has been carried out in dog ventricle (Mines 1913), aggregates of spontaneously beating embryonic chick ventricular cells (Guevara, Shrier, and Glass 1990), frog ventricle (Hall, Bahar, and Gauthier 1999), and single rabbit ventricular cells (Yehia, Jeandupeux, Alonso, and Guevara 1999).

The bistability of Figure 3.30 implies that there are two stable limit cycles present in the phase space of the system. The simplest way in which this can occur is if there is an unstable limit cycle also present, with its stable manifold (vase-shaped surface in Figure 3.31) acting as the separatrix between the basins of attraction of the two stable limit cycles. Suppose that as a parameter is changed, there is a reverse saddle-node bifurcation of periodic cycles, destroying the unstable saddle limit cycle and one of the two stable nodal limit cycles. In that case, bistability would no longer

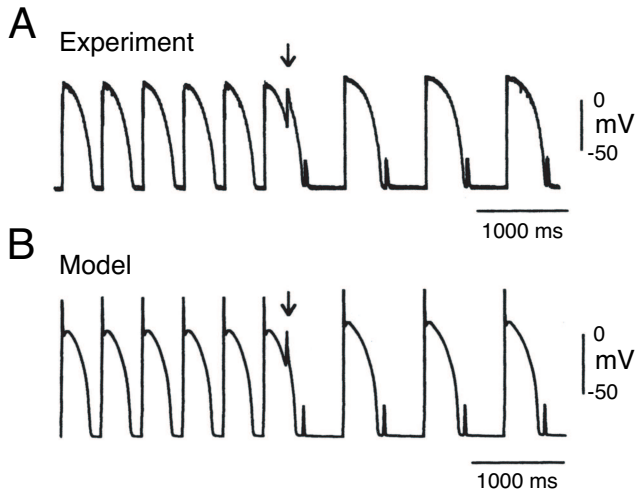

Figure 3.30. Bistability between 1:1 and 2:1 rhythms in (A) a periodically driven single cardiac cell isolated from the rabbit ventricle, (B) an ionic model of ventricular membrane. From Yehia, Jeandupeux, Alonso, and Guevara (1999).

be present, since there would be only a single limit cycle left in the phase space of the system, which would be stable, resulting in monostability.

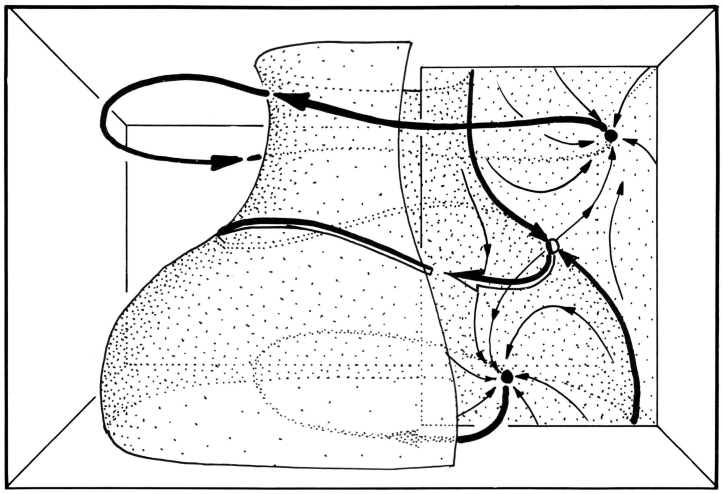

Figure 3.31. Coexistence of two stable (nodal) limit cycles, producing bistability of periodic orbits. Cycle in middle of picture is unstable (saddle) limit cycle. From Abraham and Shaw (1982).

3.6 Period-Doubling Bifurcation of Limit Cycles

3.6.1 Physiological Examples of Period-Doubling Bifurcations

Figure 3.32 shows an example of a period-doubling bifurcation in a single cell isolated from the rabbit ventricle that is subjected to periodic driving with a train of current pulses. As the interval between stimuli is decreased, the 1:1 rhythm (Figure 3.32A), in which each stimulus pulse produces an identical action potential, is replaced with an alternans or 2:2 rhythm (Figure 3.32B), in which two different morphologies of action potential are produced, which alternate in a beat-to-beat fashion. Figure 3.33 shows similar behavior in an ionic model of ventricular membrane.

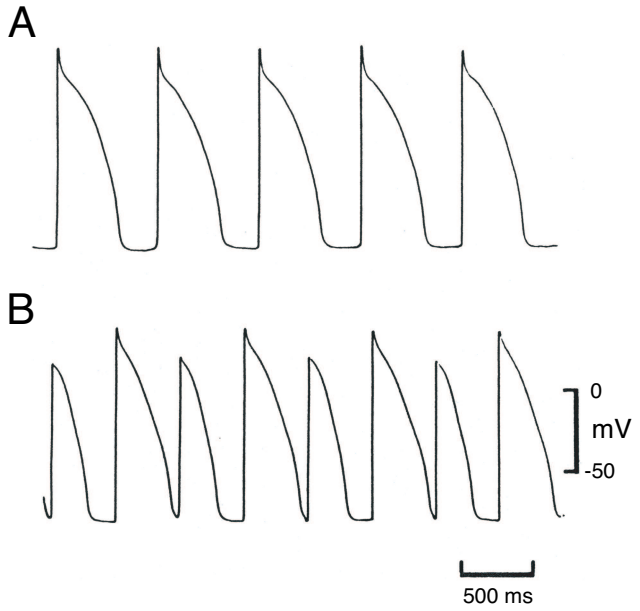

Figure 3.32. Periodic stimulation of a single rabbit ventricular cell results in (A) 1:1 or (B) 2:2 rhythm. From Guevara et al. (1989).

Another example from electrophysiology involves periodic driving of the membrane of the squid giant axon with a train of subthreshold current pulses (Figure 3.34). As the interval between pulses is increased, there is a direct transition from a 1:0 rhythm, in which there is a stereotypical subthreshold response of the membrane to each stimulus pulse, to a 2:0 response, in which the morphology of the subthreshold response alternates from stimulus to stimulus. One can also obtain responses similar to those seen in the experiments on the squid (Figure 3.34) in a reduced two-variable model, the FitzHugh–Nagumo equations (Kaplan et al. 1996).

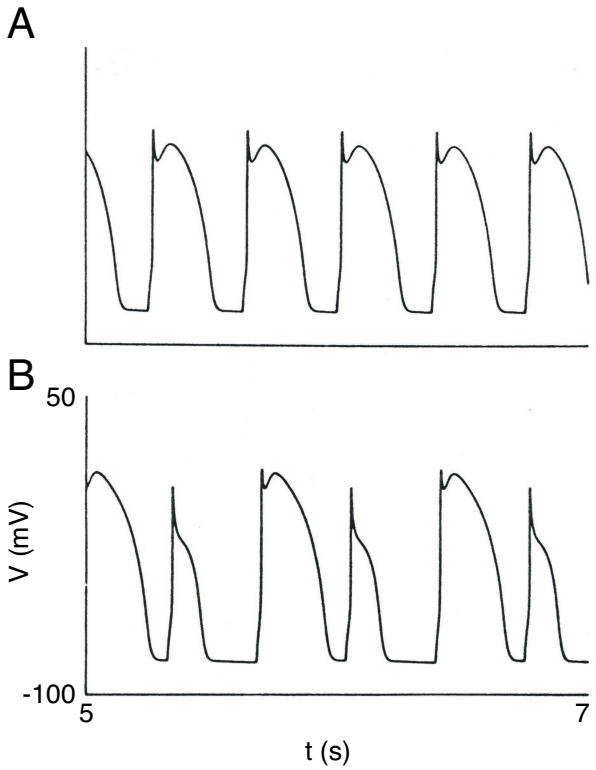

Figure 3.33. (A) 1:1 and (B) 2:2 rhythms in an ionic model of ventricular membrane. From Guevara et al. (1989).

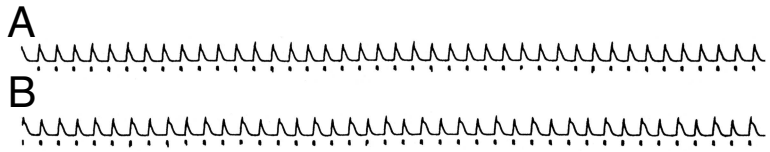

Figure 3.34. (A) 1:0 and (B) 2:0 subthreshold responses of the giant axon of the squid. From Kaplan et al. (1996).

3.6.2 Theory of Period-Doubling Bifurcations of Limit Cycles

In the two examples shown just above, as a parameter is changed, a periodic rhythm is replaced by another periodic rhythm of about twice the period of the original rhythm. In fact, a period-doubling bifurcation has taken place in both cases. When a period-doubling bifurcation occurs, a limit cycle reverses its stability, and in addition, a new limit cycle appears in its immediate neighborhood (Figure 3.35). This new cycle has a period that is twice as long as that of the original cycle. We have previously encountered

the period-doubling bifurcation in the setting of a one-dimensional finite-difference equation (Chapter 2). In that case, a period-1 orbit is destabilized and a stable period-2 orbit produced.

Note that a period-doubled orbit cannot exist in an ordinary differential equation of dimension less than three, since otherwise, the trajectory would have to cross itself, thus violating uniqueness of solution. The trajectories and orbits shown in Figure 3.35 are thus projections onto the plane of trajectories in a three- or higher-dimensional system.

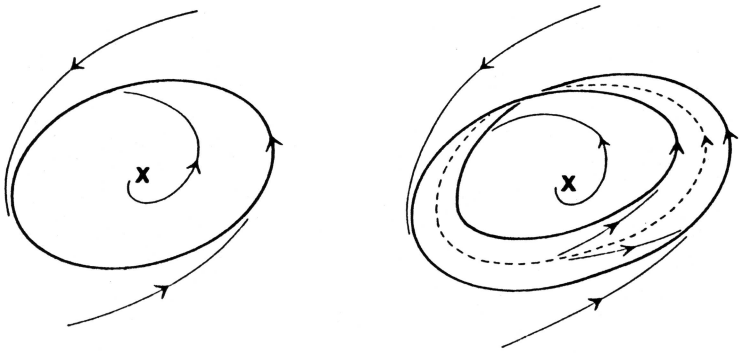

Figure 3.35. Period-doubling bifurcation of a limit cycle. From Guevara and Jongsma (1992).

A period-doubling bifurcation can be supercritical, as shown in Figure 3.35, or subcritical. Figure 3.36 gives the two corresponding bifurcation diagrams.

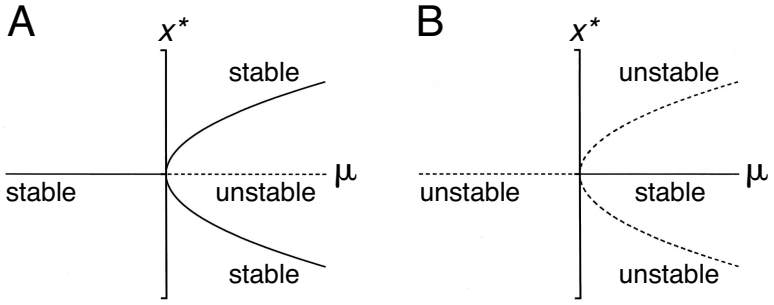

Figure 3.36. Bifurcation diagram of period-doubling bifurcation: (A) Supercritical bifurcation, (B) Subcritical bifurcation.

3.6.3 Floquet Multipliers at the Period-Doubling Bifurcation

A limit cycle undergoes a period-doubling bifurcation when one of its real Floquet multipliers passes through -1 on the unit circle (Figure 3.37A). To appreciate this fact, we must first understand how it is possible to have a negative Floquet multiplier. A negative Floquet multiplier implies, for a limit cycle in a two-dimensional system, that the slope of the return map must be negative. This means that a trajectory that has just intersected the Poincaré plane of section must next pierce the plane of section, which is a one-dimensional curve in a two-dimensional system, at a point on the other side of the limit cycle (Figure 3.37B). This cannot happen for a two-dimensional system defined in the plane, since to do so the trajectory would have to cross the limit cycle itself, thus violating uniqueness of solution. One way that this can happen in a two-dimensional system is if the orbit is a twisted orbit lying in a Möbius band. If the orbit is stable, the multiplier lies in the range $(-1, 0)$ (Figure 3.37C), while if it is unstable, it is more negative than -1 (Figure 3.37D).

Figure 3.38 shows a period-doubled cycle in a three-dimensional system. Also illustrated is the destabilized original cycle, which is a saddle cycle. In contrast to the case of bistability of periodic orbits (Figure 3.31), the stable manifold of the saddle cycle is twisted.

Perhaps the most interesting fact about the period-doubling bifurcation is that a cascade of such bifurcations can lead to chaotic dynamics. We have already encountered this in the setting of finite-difference equations (see Chapter 2). Figure 3.39 shows an example of this route to chaos in the much-studied Rössler equations:

$$\frac{dx}{dt} = -y - z, \tag{3.9a}$$

$$\frac{dy}{dt} = x + ay, \tag{3.9b}$$

$$\frac{dz}{dt} = b + xz - cz. \tag{3.9c}$$

As the parameter c in this system of three-dimensional ordinary differential equations is changed, the limit cycle (Figure 3.39A-A)undergoes a sequence of successive period-doublings (Figures 3.39A-B-D) that eventually results in the production of several chaotic **strange attractors** (Figures 3.39A-E-H show 8-, 4-, 2- and 1-banded attractors). Figure 3.39B gives the largest Lyapunov exponent as a function of c. Remember that a positive Lyapunov exponent is evidence for the existence of chaotic dynamics (see Chapter 2). Figure 3.39C gives a return map extracted by plotting successive maxima of the variable x for $c = 5.0$. This map is remarkably similar to the quadratic map encountered earlier (see Chapter 2).

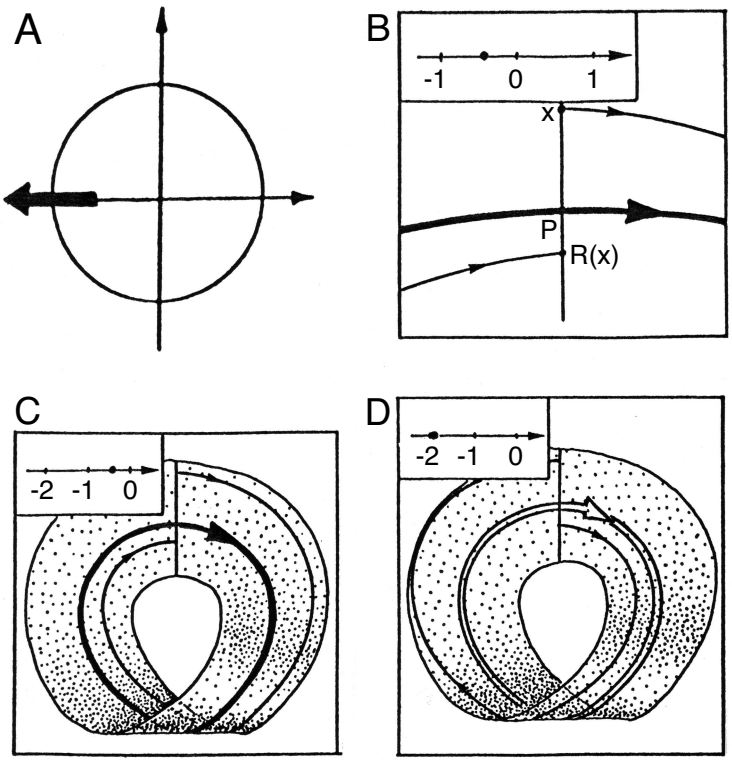

Figure 3.37. (A) Floquet diagram for period-doubling bifurcation. (B) Poincaré section of twisted cycle. (C) Stable twisted cycle. (D) Unstable twisted cycle. Panels A and B from Seydel (1994). Panels C and D adapted from Abraham and Shaw (1982).

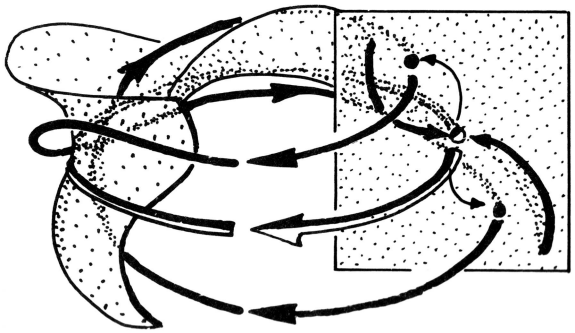

Figure 3.38. Period-doubled limit cycle in a three-dimensional system. Cycle in middle of picture is the original limit cycle, which has become destabilized. From Abraham and Shaw (1982).

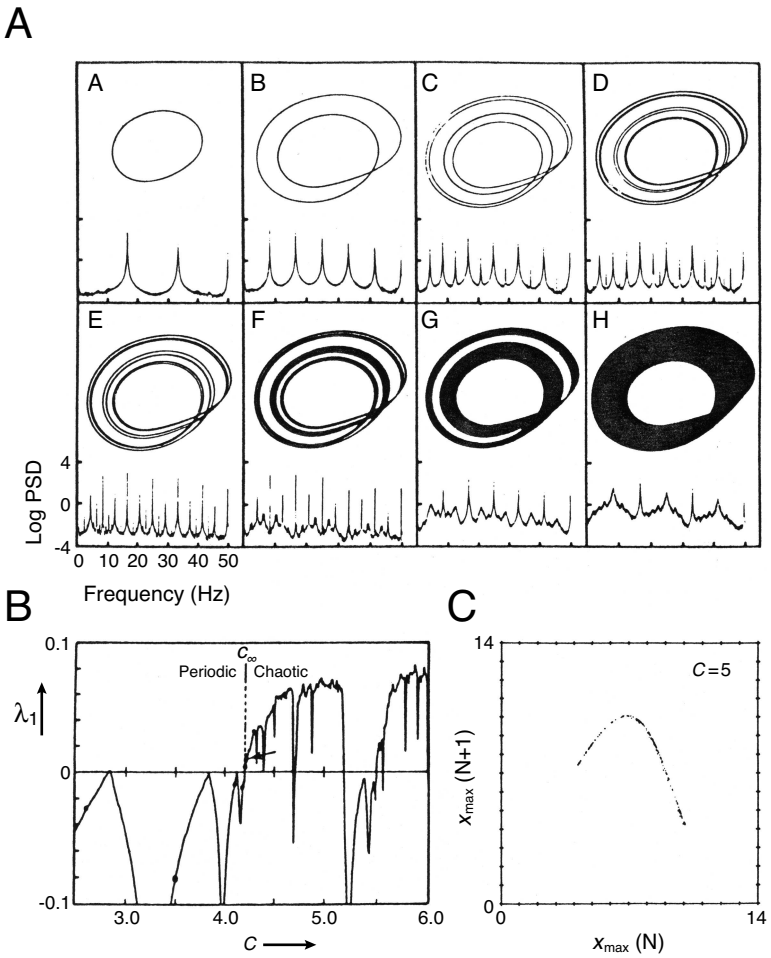

Figure 3.39. (A) Phase portraits (projections onto xy-plane) of Rössler equations (Equation 3.9), showing the cascade of period-doubling bifurcations culminating in chaotic dynamics. The power spectrum is shown below each phase portrait. (B) The largest Lyapunov number (λ_1) is given as a function of the bifurcation parameter, c. (C) Return map for strange attractor existing at $c = 5.0$. Adapted from Crutchfield et al. (1980) and Olsen and Degn (1985).

3.7 Torus Bifurcation

In a **torus bifurcation**, a spiral limit cycle reverses its stability and spawns a zero-amplitude torus in its immediate neighborhood, to which trajectories in the system are asymptotically attracted or repelled. The amplitude of the torus grows as the bifurcation parameter is pushed further beyond the bifurcation point. Figure 3.40 shows a supercritical torus bifurcation

in a three-dimensional system. One starts off with a stable spiral limit cycle, whose Floquet multipliers are therefore a complex-conjugate pair lying within the unit circle (Figure 3.40A). Beyond the bifurcation point (Figure 3.40B), the trajectories in the system are now asymptotically attracted to orbits on the two-dimensional surface of a torus. These orbits can be either periodic or quasiperiodic. Note that the original limit cycle still exists, but that it has become an unstable spiral cycle, with a complex-conjugate pair of Floquet multipliers now lying outside of the unit circle (Figure 3.40B). A torus bifurcation thus occurs when a complex-conjugate pair of Floquet multipliers crosses the unit circle (Figure 3.40C). Figure 3.41 gives the bifurcation diagram.

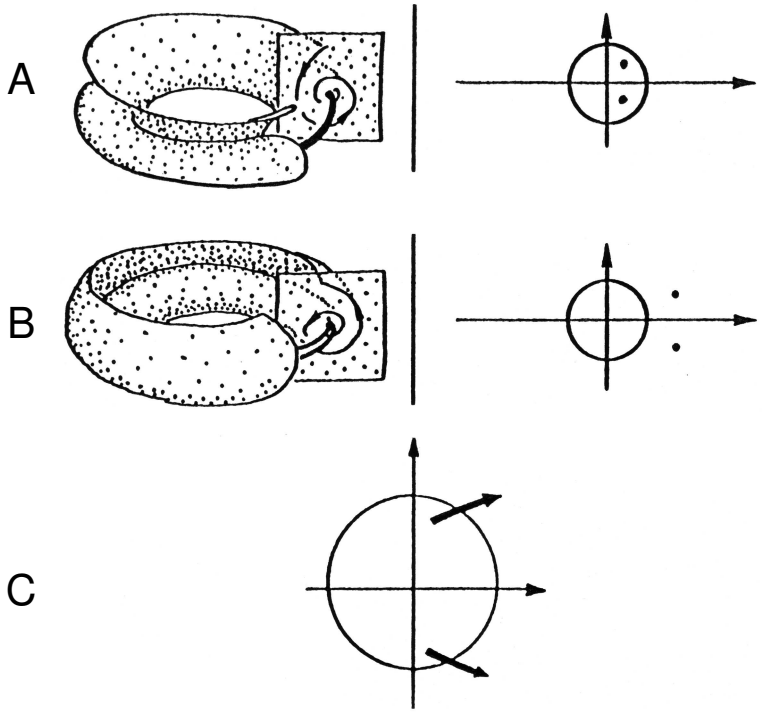

Figure 3.40. The torus bifurcation in a three-dimensional system. (A) A stable spiral limit cycle and its Floquet diagram. (B) Unstable limit cycle produced as a result of torus bifurcation. (C) Floquet multipliers crossing through unit circle at torus bifurcation point. Panels A (left) and B (left) adapted from Abraham and Shaw (1982). Panels A (right), B (right) and C adapted from Seydel (1994).

To understand why at a torus bifurcation a pair of complex-conjugate Floquet multipliers goes through the unit circle (Figure 3.40C), we must consider the significance of a Floquet multiplier being a complex number. Before the torus bifurcation occurs, when we have a stable spiral cycle (Fig-

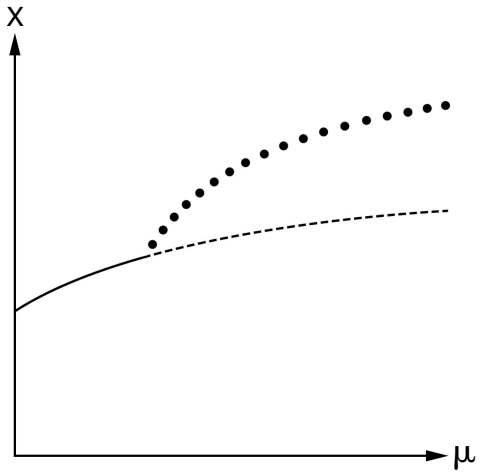

Figure 3.41. Bifurcation diagram of supercritical torus bifurcation. *Solid curve*: stable limit cycle, *dashed curve*: unstable limit cycle, *filled circles*: attracting torus.

ure 3.40A), the presence of a complex pair of multipliers within the unit circle means that the fixed point in the two-dimensional Poincaré return map is a stable spiral point (Figure 3.42A). The torus bifurcation of the orbit corresponds to a Hopf bifurcation in the map, which converts the stable spiral fixed point of the map into an unstable spiral point, spawning an **invariant circle** in its neighborhood (Figure 3.42B). This invariant circle corresponds to the piercing of the Poincaré plane of section by a quasiperiodic orbit lying in the surface of the torus that asymptotically visits all points on the circle. Because of its association with a Hopf bifurcation on the return map, the torus bifurcation is also called a **Hopf bifurcation of periodic orbits** or a **secondary Hopf bifurcation**. It is also referred to as the **Hopf–Neimark** or **Neimark bifurcation.** (Note: This description of a torus bifurcation in terms of bifurcations involving its return map is a bit simplistic, since one can have periodic as well as quasiperiodic orbits generated on the torus.) While we have illustrated the supercritical torus bifurcation above, subcritical torus bifurcations, in which an unstable limit cycle stabilizes and a repelling torus is born, also exist.

Several examples of quasiperiodic behavior have been found in biological systems. In particular, quasiperiodicity occurs naturally when one considers the weak forcing of an oscillator (see Chapter 5) or the weak interaction of two or more oscillators. In these cases, the quasiperiodic behavior arises out of a torus bifurcation (Schreiber, Dolnik, Choc, and Marek 1988).

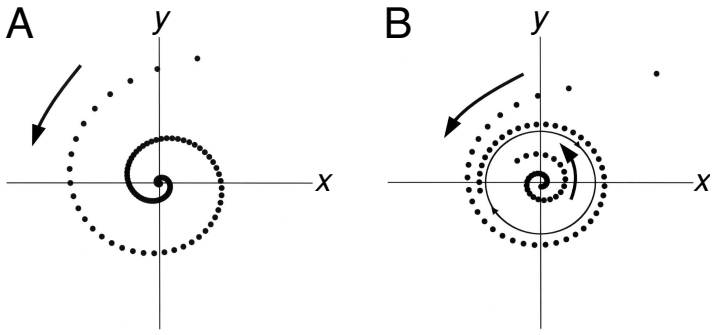

Figure 3.42. (A) Stable spiral point on Poincaré return map of original stable spiral limit cycle. (B) Invariant circle of Poincaré return map produced by Hopf bifurcation.

3.8 Homoclinic Bifurcation

A limit cycle is stable if all of its nontrivial Floquet multipliers lie within the unit circle. If a parameter is gradually changed, the limit cycle can lose its stability in a "local" bifurcation if and only if one or more of these multipliers crosses through the unit circle. This can happen in one of only three generic ways as a single bifurcation parameter is changed: A single real multiplier goes through $+1$ (saddle-node bifurcation); a single real multiplier goes through -1 (period-doubling bifurcation); or a pair of complex-conjugate multipliers crosses through the unit circle (torus bifurcation). However, there are other (nonlocal) bifurcations in which limit cycles can be created or destroyed. We now turn to consideration of one of these "global" bifurcations: the homoclinic bifurcation.

A **heteroclinic connection** is a trajectory connecting two different fixed points (thick horizontal line in Figure 3.43A). It takes an infinite amount of time to traverse the connection: The amount of time taken to leave the starting point of the connection grows without limit as one starts closer to it, while the amount of time taken to approach more closely the terminal point of the connection also grows without limit. A **heteroclinic cycle** is a closed curve made up of two or more heteroclinic connections (e.g., Figure 3.43B). To cause confusion, the term **heteroclinic orbit** has been used to denote either a heteroclinic connection or a heteroclinic cycle. We shall not use it further.

A **homoclinic orbit** is a closed curve that has a single fixed point lying somewhere along its course. Perhaps the simplest example is the case in a two-dimensional system in which the homoclinic orbit involves a saddle point (Figure 3.44A). The homoclinic orbit is formed when one of the pair of separatrices associated with the stable manifold of the saddle point coincides with one of the pair of trajectories forming its unstable manifold (Figure 3.44B). As with the heteroclinic cycle, the homoclinic orbit is of

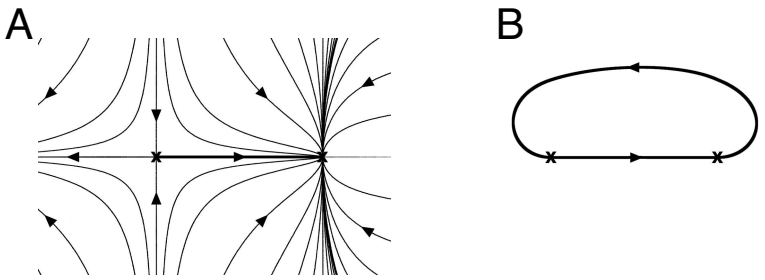

Figure 3.43. (A) Heteroclinic connection. (B) Heteroclinic cycle.

infinite period. (By continuity, it is clear that there must be some other fixed point(s) and/or limit cycle(s) present within the interior of the homoclinic orbit of Figure 3.44B.) Another type of homoclinic orbit that can occur in higher-dimensional systems is illustrated in Figure 3.44C. Here, in a three-dimensional system, the fixed point is a saddle-focus, having a pair of complex eigenvalues with positive real part, and a single real negative eigenvalue. Homoclinic orbits are not structurally stable: i.e., an infinitesimally small change in any system parameter will generally lead to their destruction, which can then result in the appearance of a periodic orbit (the homoclinic bifurcation that we shall now discuss) or chaotic dynamics (e.g., **Shil'nikov chaos**; see Guevara 1987; Guevara and Jongsma 1992; Wiggins 1988; Wiggins 1990).

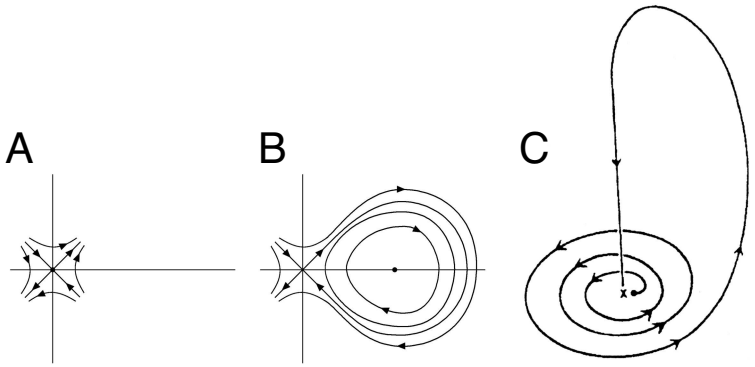

Figure 3.44. (A) Saddle point in a two-dimensional ordinary differential equation. (B) Homoclinic orbit involving a saddle point in a two-dimensional ordinary differential equation. (C) Homoclinic orbit involving a saddle focus in a three-dimensional ordinary differential equation. Panel C from Guevara and Jongsma 1992.

In one example of the homoclinic bifurcation in a two-dimensional system, there are initially two fixed points, one of which is a saddle point, and the other an unstable spiral point. There are no limit cycles present.

As a bifurcation parameter is changed, the curved trajectory associated with one of the separatrices of the unstable manifold of the saddle point approaches the trajectory associated with its stable manifold that spirals out of the unstable spiral point. At the bifurcation point, these two trajectories coincide, producing a homoclinic orbit (the closed curve starting and terminating on the saddle point). Just beyond the bifurcation point, the homoclinic orbit disappears, and is replaced by a stable limit cycle. Thus, the net result of the bifurcation is to produce a stable limit cycle, since the two preexisting fixed points remain. A homoclinic bifurcation can also result in the appearance of an unstable limit cycle (simply reverse the direction of all the arrows on the trajectories in the case described above).

There are several examples of homoclinic bifurcations in biological systems. Figure 3.45 is an example drawn from an ionic model of the sinoatrial node. As an increasingly large hyperpolarizing (positive) bias current is injected, the period of the limit cycle (T), which corresponds to the interval between spontaneously generated action potentials, gradually prolongs from its normal value of about 300 ms. At $I_{\text{bias}} \approx 0.39 \mu\text{A/cm}^2$, there is a homoclinic bifurcation, where $T \to \infty$. This bifurcation is heralded by a pronounced increase in the rate of growth of the period of the orbit as the bifurcation point is approached. This is a feature that distinguishes the homoclinic bifurcation from the other bifurcations we have studied so far involving periodic orbits (Hopf, saddle-node, period-doubling, and torus bifurcations). Another characteristic of the homoclinic bifurcation is that the periodic orbit appears at large (i.e., finite) amplitude. Of the other bifurcations of periodic orbits considered thus far, this feature is shared only with the saddle-node bifurcation.

3.9 Conclusions

A mathematical appreciation of physiological dynamics must deal with the analysis of the ways in which fixed points and oscillations can become stabilized or destabilized as parameters in physiological systems are changed. Over the years, there have been a vast number of purely experimental studies that document these sorts of dynamic changes. Many such studies are phenomenological and contain descriptions of remarkable dynamical behaviors. These papers now lie buried in dusty libraries, perhaps permanently lost to the explosion of new information technologies that has left many classical papers "off-line."

In this chapter we have illustrated some of the simplest types of bifurcations and shown biological examples to illustrate these phenomena. We have discussed three elementary one-parameter bifurcations involving fixed points alone (saddle-node, pitchfork, transcritical) as well as one two-parameter bifurcation (cusp catastrophe). We have also studied the three

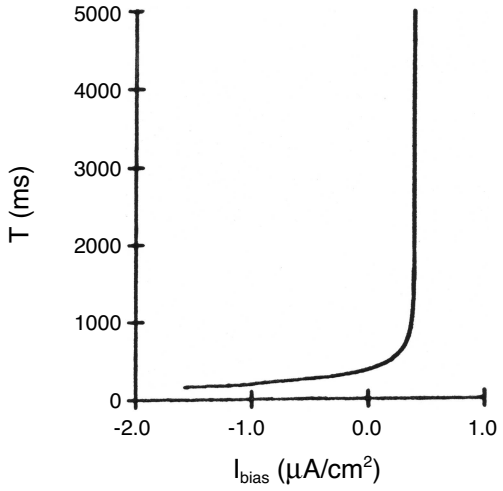

Figure 3.45. Bifurcation diagram giving period of limit cycle when a homoclinic bifurcation occurs in an ionic model of the sinoatrial node. From Guevara and Jongsma (1992).

local bifurcations of a limit cycle (saddle-node, period-doubling, torus) as well as one global bifurcation (homoclinic). Most work in physiology has centered on the local bifurcations. While there has been relatively little work on global bifurcations, one can anticipate that this will change in the future. Several other bifurcations are known to exist (Wiggins 1990), but have not yet generally shown up in modeling work on biological systems.

3.10 Problems

1. In a negative-feedback system, control mechanisms are present that act to reduce deviations from a set-point. For example, in a synthetic pathway with end-product inhibition, each substance is converted into a new substance, but the rate of synthesis of the initial product is a sigmoidally decreasing function of the concentration of the last product in the pathway. This problem illustrates the basic concept that an oscillation can be produced in a negative-feedback system by either increasing the gain of the negative feedback (the higher the value of m in equation (3.10), the higher the gain) or by increasing the time delay; see, for example, Goodwin (1963). The oscillation arises as a consequence of a pair of complex-conjugate eigenvalues crossing the imaginary axis (a Hopf bifurcation; see Chapter 2). In this context, the multiple steps of the synthetic pathway induce a delay in the feedback. However, in other circumstances, such as the control of

blood-cell production (see Chapter 8) or the control of pupil diameter (see Chapter 9), it may be more appropriate to represent the time delay in a negative-feedback system using a time-delay differential equation.

To illustrate the properties of negative-feedback systems, we consider a simple model equation

$$\begin{aligned} \frac{dx_1}{dt} &= \frac{0.5^m}{0.5^m + x_N^m} - x_1, \\ \frac{dx_i}{dt} &= x_{i-1} - x_i, \quad i = 2, 3, \ldots, N, \end{aligned} \tag{3.10}$$

where m is a parameter (often called the Hill coefficient) controlling the steepness of the negative feedback, N is the number of steps in the pathway, and x and y are nonnegative.

Determine the conditions for the fixed point at $x_i = 0.5$, $i = 1-N$ to be stable as a function of m and N. In this problem if you carry through the computations until $N = 7$, the mathematics indicates the possibility for a second pair of complex eigenvalues crossing the imaginary axis as m is increased. Based on your theoretical understanding of the stability of fixed points, do you expect this second bifurcation to have an effect on the observed dynamics?

An interesting project is to carry out numerical integration of this equation to compare the theoretically predicted boundaries for stability of the fixed points with the numerically computed values. Write a program in `Matlab` or `XPP` to numerically study the behavior of equation (3.10), and determine whether there is any effect on the dynamics when the second pair of eigenvalues crosses the unit circle for $N = 7$ as m increases.

2. The "Brusselator" is a toy chemical reaction scheme (Prigogine and Lefever 1968) given by

$$\begin{aligned} A &\longrightarrow X, \\ 2X + Y &\longrightarrow 3X, \\ B + X &\longrightarrow Y + D, \\ X &\longrightarrow E. \end{aligned}$$

Given some assumptions, the dynamic equations governing these reactions are given by

$$\begin{aligned} \frac{dx}{dt} &= A + Kx^2y - Bx - x = f(x, y), \\ \frac{dy}{dt} &= -Kx^2y + Bx = g(x, y), \end{aligned}$$

where x, y, A, B, and K are nonnegative. Pick $K = 1$.

(a) Determine the fixed points of the Brusselator.

(b) Characterize the nature of the fixed points and their stability as the parameter B is varied. Does a Hopf bifurcation ever occur? If so, at what value of B? What is the Hopf period at this value of B?
(c) Sketch the phase portrait of the Brusselator for various regions of the B versus A parameter space (don't forget that A and B are nonnegative).
(d) Write a `Matlab` or `XPP` program to numerically investigate the Brusselator and see how well your analytic predictions match what is seen experimentally.

3. (This problem is based on the paper by Lengyel and Epstein 1991.) Assume that two Brusselators are connected by a semipermeable membrane (that allows both x and y to diffuse down their concentration gradients), so that the dynamics in each compartment [1 and 2] are governed by

$$\begin{aligned}
\frac{dx_1}{dt} &= f(x_1, y_1) + D_x(x_2 - x_1),\\
\frac{dy_1}{dt} &= g(x_1, y_1) + D_y(y_2 - y_1),\\
\frac{dx_2}{dt} &= f(x_2, y_2) + D_x(x_1 - x_2),\\
\frac{dy_2}{dt} &= g(x_2, y_2) + D_y(y_1 - y_2).
\end{aligned}$$

(a) Are there parameter values such that each Brusselator is stable, but coupling them together produces an instability?
(b) Characterize the nature of the instability as completely as possible.
(c) Modify the program you wrote for the previous problem to numerically investigate the behavior of the diffusively coupled Brusselators. How well do your analytic predictions match what you observe numerically?

3.11 Computer Exercises: Numerical Analysis of Bifurcations Involving Fixed Points

In these computer exercises, which involve the use of the `Auto` feature of `XPP`,[‡] we will carry out bifurcation analysis on three different simple one-dimensional ordinary differential equations.

[‡]See Introduction to `XPP` in Appendix A.

Ex. 3.11-1. **Bifurcation Analysis of the Transcritical Bifurcation**

The first equation we study is

$$\frac{dx}{dt} = x(\mu - x). \tag{3.11}$$

The object of this exercise is to construct the bifurcation diagram of equation (3.11), with x being the **bifurcation variable**, and μ the **bifurcation parameter**. The file **xcrit.ode** is the `XPP` file containing the instructions for integrating the above equation.

(a) **Finding the Fixed Points.** Start `XPP` and select the main `XPP` window (titled `XPP >> xcrit.ode`). After turning the bell off (in the `File` menu), start the numerical integration. You will then see a plot of the variable x as a function of time. There appears to be a stable fixed point at $x = 0$.

To investigate this further, make runs from a range of initial conditions. In the `Range Integrate` menu, change `Steps` to 40, `Start` to -2, `End` to 2. In the plot window, one now sees the result of starting at 40 different initial conditions x_0 evenly spaced between $x = -2$ and $x = 2$.

The runs starting with $x_0 = 0$ and $x_0 = -1$ show that both of these points are fixed points. All initial conditions on the interval $(-1, 2]$ (in fact, $(-1, \infty)$) are attracted to the stable fixed point at $x = 0$, while those starting from $x < -1$ go off to $-\infty$. Thus, $x = -1$ is an unstable fixed point.

(b) **Effect of changing μ.** Now investigate the effect of changing the bifurcation parameter μ from -1 (the default value assigned in `xcrit.ode`) to $+1$.
Has anything happened to the location of the fixed points or to their stability?
Repeat the above for $\mu = 0$.
How many fixed points are now present and what can you say about their stability?

The above method of finding fixed points and their stability using brute-force numerical integration, visual inspection of the many traces that result, and repeated change of parameter is very tedious. It makes far more sense to determine the location of a fixed point at one value of the parameter and then to follow it as the parameter is changed using some sort of continuation technique (Seydel 1988). This is exactly what `Auto` does.

(c) **Plotting the bifurcation diagram with `Auto`.** When you have opened the `Auto` window, change `Xmin` and `Ymin` to -12,

and `Xmax` and `Ymax` to 12. In the `AutoNum` window that pops up, change `Par Min` to -10 and `Par Max` to 10 (this sets the range of μ that will be investigated). Also change `NPr` to 200 and `Norm max` to 20.

We now have to give `Auto` a seed from which to start. Set $\mu = -10.0$ in the `XPP` window `Parameters`, and set $x = -10.0$ in the `Initial Data` window. Now go back to the `It's Auto man!` window and select `Run` and click on `Steady state`.

A bifurcation curve with two branches, consisting of two intersecting straight lines, will now appear on the plot.
One can save a copy of the bifurcation diagram as a PostScript file to be printed out later.

(d) **Studying points of interest on the bifurcation diagram.** The numerical labels 1 to 5 appear on the plot, identifying points of interest on the diagram. In addition, `Auto` prints some relevant information about these labels in the xterm window from which `XPP` was invoked.

In this case, the point with label LAB = 1 is an endpoint (EP), since it is the starting point; the point with LAB = 2 is a branch-point (BP), and the points with LAB = 3, 4, and 5 are endpoints of the branches of the diagram. The points lying on the parts of the branches between LAB = 2 and 5 and betwen LAB = 2 and 3 are stable, and thus are indicated by a thick line. In contrast, the other two segments between 1 and 2 and between 2 and 4 are plotted as thin lines, since they correspond to unstable fixed points. Inspect the points on the bifurcation curve by clicking on `Grab` in the main `Auto` window.

Verify that the eigenvalue lies outside of the unit circle for the first 34 points on Branch 1 of the bifurcation diagram. At point 34, the eigenvalue crosses into the unit circle, and the point becomes stable.

Ex. 3.11-2. **Bifurcation Analysis of the Saddle-Node and Pitchfork Bifurcations.** You can now invoke `XPP` again, carry out a few integration runs over a range of initial conditions, and obtain the bifurcation diagrams for two other files, suggestively named **saddnode.ode** and **pitchfork.ode**. The former is for the equation

$$\frac{dx}{dt} = \mu - x^2, \tag{3.12}$$

while the latter is for

$$\frac{dx}{dt} = x(\mu - x^2). \tag{3.13}$$

Remember that before you run `Auto`, you must specify a valid starting point for the continuation: Calculate and enter the steady-state value of x (in the `Initial Data` window) appropriate to the particular value of μ being used (in the `Parameters` window). If "X out of bounds" error occurs, this means that x has become too large or too small. Use `Data Viewer` window to see whether x is heading toward $+\infty$ or $-\infty$.

3.12 Additional Computer Exercises

Additional computer exercises involving the material presented in this chapter appear at the end of Chapter 4, Dynamics of Excitable Cells, in the context of models of excitable membrane.